Quinazolinone Derivatives as Orally Available Ghrelin Receptor Antagonists for the Treatment of Diabetes and Obesity

Joachim Rudolph,*,† William P. Esler,*,‡ Stephen O'Connor,† Philip D. G. Coish,† Philip L. Wickens,† Michael Brands,†
Donald E. Bierer,† Brian T. Bloomquist,‡ Georgiy Bondar,† Libing Chen,† Chih-Yuan Chuang,† Thomas H. Claus,‡ Zahra Fathi,‡
Wenlang Fu,† Uday R. Khire,† James A. Kristie,§ Xiao-Gao Liu,† Derek B. Lowe,† Andrea C. McClure,† Martin Michels,†
Astrid A. Ortiz,‡ Philip D. Ramsden,† Robert W. Schoenleber,† Tatiana E. Shelekhin,† Alexandros Vakalopoulos,†
Weifeng Tang,§ Lei Wang,† Lin Yi,† Stephen J. Gardell,‡ James N. Livingston,‡ Laurel J. Sweet,‡ and William H. Bullock†

*Departments of Chemistry Research, Metabolic Disorders Research, and Research Technologies, Bayer Pharmaceuticals Corporation,
400 Morgan Lane, West Haven, Connecticut 06516*

The peptide hormone ghrelin is the endogenous ligand for the type 1a growth hormone secretagogue receptor (GHS-R1a) and the only currently known circulating appetite stimulant. GHS-R1a antagonism has therefore been proposed as a potential approach for obesity treatment. More recently, ghrelin has been recognized to also play a role in controlling glucose-induced insulin secretion, which suggests another possible benefit for a GHS-R1a antagonist, namely, the role as an insulin secretagogue with potential value for diabetes treatment. In our laboratories, piperidine-substituted quinazolinone derivatives were identified as a new class of small-molecule GHS-R1a antagonists. Starting from an agonist with poor oral bioavailability, optimization led to potent, selective, and orally bioavailable antagonists. In vivo efficacy evaluation of selected compounds revealed suppression of food intake and body weight reduction as well as glucose-lowering effects mediated by glucose-dependent insulin secretion.

Introduction

It is estimated that currently some 194 million people worldwide, or 5.1% in the adult population, have diabetes and that this will increase to 333 million, or 6.3%, by 2025. It is the fourth or fifth leading cause of death in most developed countries, and there is substantial evidence that it is an epidemic in many developing and newly industrialized nations.[1]

Obesity is the principal risk factor for type 2 diabetes. In western countries, around 90% of type 2 diabetes cases are attributable to weight gain, and childhood overweight issues and obesity are now leading to an emergence of premature type 2 diabetes, which is particularly difficult to manage once established.[1] While even modest reductions in body weight and/or adiposity have been shown to result in marked improvements in insulin sensitivity or even elimination of diabetic symptoms, weight loss is more difficult to achieve in diabetic individuals.[1] To further complicate matters, many anti-diabetic therapies are prone to increase body weight.[2] New treatments that act directly to improve glucose tolerance while simultaneously promoting clinically meaningful weight loss could have tremendous value for therapeutic intervention in type 2 diabetes.

Ghrelin, an acylated peptide hormone predominantly produced in the stomach, is the natural ligand of the growth hormone secretagogue receptor type 1a (GHS-R1a).[a] Because of its recently recognized role as a powerful orexigenic (appetite stimulant), ghrelin has attracted high interest over the past few years.[3−5] On the basis of numerous studies on ghrelin in humans and animals, its main function is regarded to be acute meal initiation as well as long-term energy-balance and body-weight regulation. Consequently, ghrelin blockade by GHS-R1a antagonists has been put forth as a new concept for treating obesity, and several pharmaceutical companies have recently revealed activity in this area.[6]

While much of the literature on ghrelin has focused on its effect on food intake, a growing body of data suggests that ghrelin and its receptor play a direct role on the regulation of glucose homeostasis. Ghrelin as well as its receptor GHS-R1a are detectable in islet cells,[7−13] and ghrelin has been found to suppress insulin secretion in multiple islet model systems.[11,12,14,15] The physiological relevance of this effect to glucose homeostasis in animals and humans has been demonstrated by numerous studies that show a clear negative correlation between ghrelin levels and insulin secretion.[12,16−25] Furthermore, peptide GHS-R1a antagonists were found to block the effects of endogenous ghrelin, to promote insulin secretion from isolated rat islets, and to increase insulin secretion and improve glucose tolerance in mice,[12] but this effect has so far not been reported with selective small molecule GHS-R1a antagonists.

A GHS-R1a receptor high-throughput screen conducted in our laboratories identified the quinazolinone derivative **1** as hit with high GHS-R1a affinity (K_i = 36 nM). Functional activity testing of this compound in a guanosine 5-*O*-(3-thiotriphosphate) (GTPγS) binding assay revealed agonistic instead of the desired antagonistic functional activity. As part of our initial structure−activity relationship (SAR) studies, we investigated the influence of *N*-alkylation on the piperidine nitrogen atom on functional activity. We synthesized the *N*-ethyl piperidine derivative of **1**, compound **2**,[26] and found this compound to have a dramatically different functional activity profile, namely, full antagonistic activity with high GHS-R1a affinity (K_i = 20 nM). Structurally related tertiary amine analogues were tested, which likewise exerted antagonistic GHS-R1a activity. The identified piperidine-substituted quinazolinone series constitutes a new class of
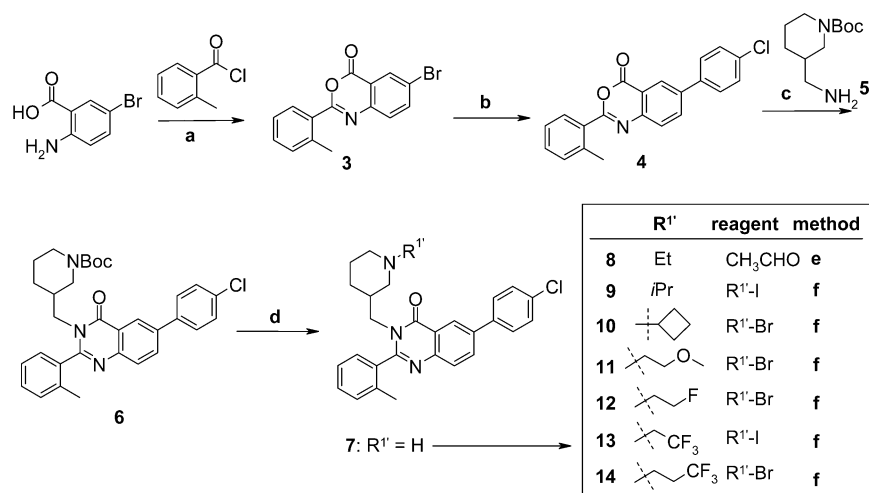
* To whom correspondence should be addressed. (J.R.) Tel: + 1 650 467 8867. Fax: + 1 650 467 8922. E-mail: rudolph.joachim@gene.com. (W.E.)Tel: +18606861256.Fax: +1860-441-0548.E-mail: william.esler@pfizer.com.
† Department of Chemistry Research.
‡ Department of Metabolic Disorders Research.
§ Department of Research Technologies.
a Abbreviations: GHS-R1a, type 1a growth hormone secretagogue receptor; GTPγS, guanosine 5-*O*-(3-thiotriphosphate); SPA, scintillation proximity assay; DIO, diet-induced obese; IPGTT, intraperitoneal glucose tolerance test.

Scheme 1[a]

	R[1']	reagent	method
8	Et	CH₃CHO	**e**
9	iPr	R[1']-I	**f**
10	cyclobutyl	R[1']-Br	**f**
11	O-methyl	R[1']-Br	**f**
12	F	R[1']-Br	**f**
13	CF₃	R[1']-I	**f**
14	CF₃	R[1']-Br	**f**

a Reagents and conditions: (a) NEt₃, CH₂Cl₂, 14 h; then Ac₂O, 50 °C, 2 h, 62%. (b) 4-Chlorophenylboronic acid, K₂CO₃, PdCl₂(dppf), 50 °C, 73%. (c) Toluene, reflux; then ethylene glycol, LiOH, 135 °C, 63%. (d) TFA, CH₂Cl₂, 82%. (e) CH₃CHO, CH₃COOH, NaB(OAc)₃H, 0 °C, 69%. (f) R″X, K₂CO₃, CH₃CN, 70 °C.

Scheme 2[a]
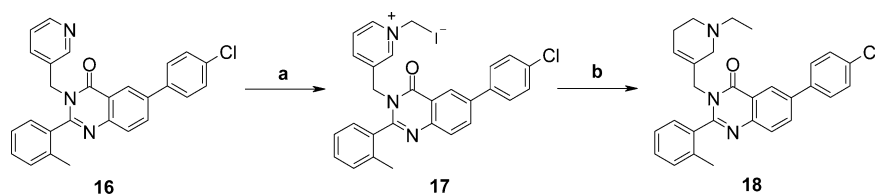
a Reagents and conditions: (a) C₂H₅I, acetone, 50 °C, 68%. (b) NaBH₄, MeOH, CH₂Cl₂, 0 °C, 17%.

GHS-R1a antagonists, unprecedented and structurally distinct from previously described GHS-R1a antagonists.[6]

1
GHSR-1a Ki = 36 nM
agonist

2
GHSR-1a Ki = 20 nM
antagonist
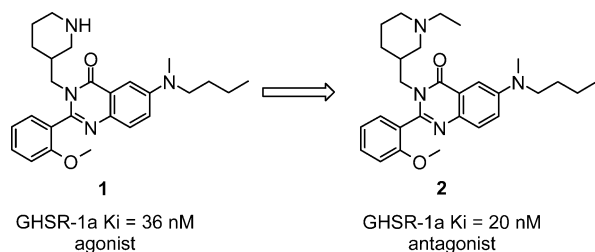
   Poor oral bioavailability is a common deficiency of most small-molecule GHS-R1a antagonists described in the literature.[6] To get a preliminary read of the pharmacokinetic behavior of our lead series, compound **2** (as its HCl salt) was orally administered to rats at a dose of 10 mg/kg. We observed low plasma exposure (C_{max} < 20 nM), which was at least partly due to high clearance. Metabolite identification studies revealed the *N*-methyl-*N*-butyl moiety as a site of significant metabolism. We therefore placed a particular focus on identifying replacements for this group.

   This account will describe systematic SAR studies on the periphery of the quinazolinone core leading to the discovery of potent GHS-R1a antagonists with favorable DMPK properties. The optimized analogues **26** and **43** are active in food intake and weight-loss models as well as in glucose tolerance animal models and represent, together with other class members, the first examples of orally available GHS-R1a antagonists with in vivo efficacy in these models.

Chemistry

   The majority of the quinazolinone analogues described in this report was synthesized according to Scheme 1. 5-Bromoanthra-

Chart 1

15
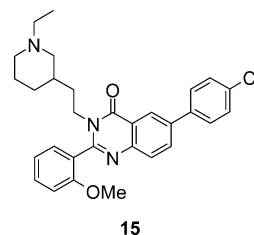
nilic acid was reacted with 2-methylbenzoylchloride to form benzoxazinone **3**.[27] Suzuki coupling and subsequent insertion[28] of BOC-protected aminomethylpiperidine **5** led to intermediate **6**, which was deprotected and subsequently alkylated using either reductive amination or nucleophilic substitution conditions to furnish compounds **8**−**14**.

   We also prepared the ethylpiperidine homologue **15**, an analogue with an extended alkyl chain, using the sequence described in Scheme 1 and appropriate starting materials (Chart 1).

   The dehydropiperidine analogue of compound **8** was synthesized as described in Scheme 2. Pyridine intermediate **16**, prepared according to the sequence described in Scheme 1, was alkylated to form pyridinium salt **17**, which was then regioselectively reduced[29] to give the dehydropiperidine derivative **18**.

   Morpholine derivative **23** was prepared from intermediate **3** and insertion of morpholine building block **19**, followed by Suzuki coupling, deprotection, and alkylation.
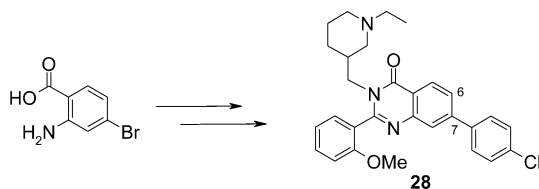
   Compounds **6**−**13** in Scheme 1 contain a chiral center at the heterocycle linkage position and were prepared as racemates. Using the sequence described in Scheme 1 and substituting the racemic piperidine building block **5** by its commercially available (*R*)- and (*S*)-enantiomers, we synthesized both enan-
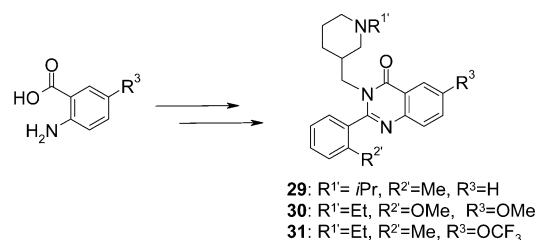
Chart 2
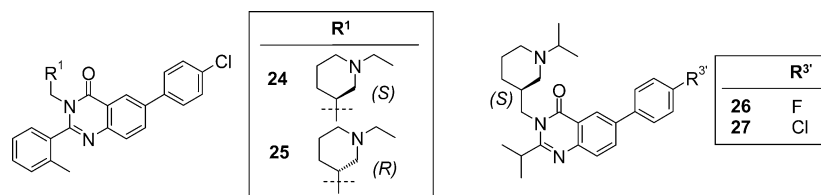
Scheme 3[a]
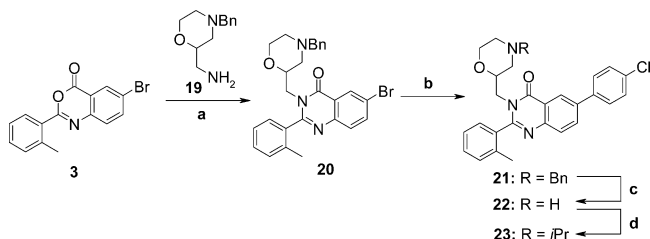
[a] Reagents and conditions: (a) Toluene, 100 °C; ethylene glycol, LiOH, 135 °C, 67%. (b) 4-Chlorophenylboronic acid, K_2CO_3, $PdCl_2(dppf)$, 90 °C, 76%. (c) 1-Chloromethyl chloroformate, CH_2ClCH_2Cl, reflux, 91%. (d) 2-Bromopropane, K_2CO_3, CH_3CN, 70 °C, 55%.

Scheme 4

Scheme 5

29: $R^{1'}= iPr$, $R^{2'}=Me$, $R^3=H$
30: $R^{1'}=Et$, $R^{2'}=OMe$, $R^3=OMe$
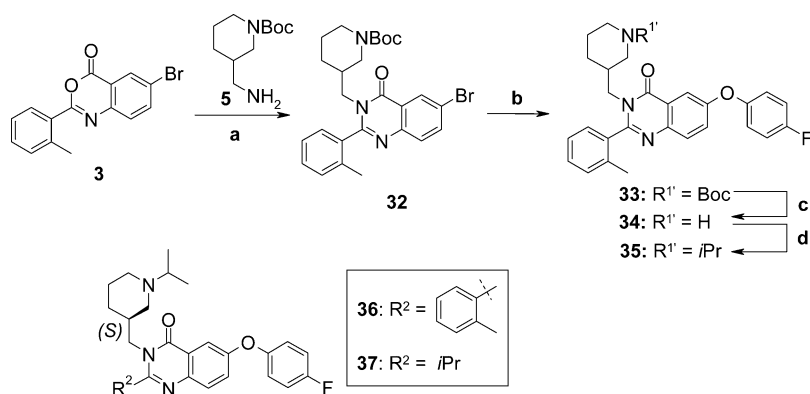**31**: $R^{1'}=Et$, $R^{2'}=Me$, $R^3=OCF_3$

tiomers of **8**, compound **24** (*S*), and compound **25** (*R*). Compounds **26** and **27** were prepared in the same fashion (Chart 2).

As part of our SAR investigation of the eastern part of the molecule, we transposed the 4-chlorophenyl side chain from the 6- to the 7-position of the quinazolinone scaffold to furnish

compound **28** (Scheme 4). This was accomplished using 2-amino-4-bromobenzoic acid instead of 2-amino-5-bromobenzoic acid as the starting material and applying otherwise analogous procedures as described in Scheme 1.

Further modification at the eastern part of the quinazolinone core included the synthesis of derivatives with truncated side chains. These compounds were synthesized from the corresponding anthranilic acids using the same sequence as described in Scheme 1 and omitting the Suzuki coupling step (Scheme 5).
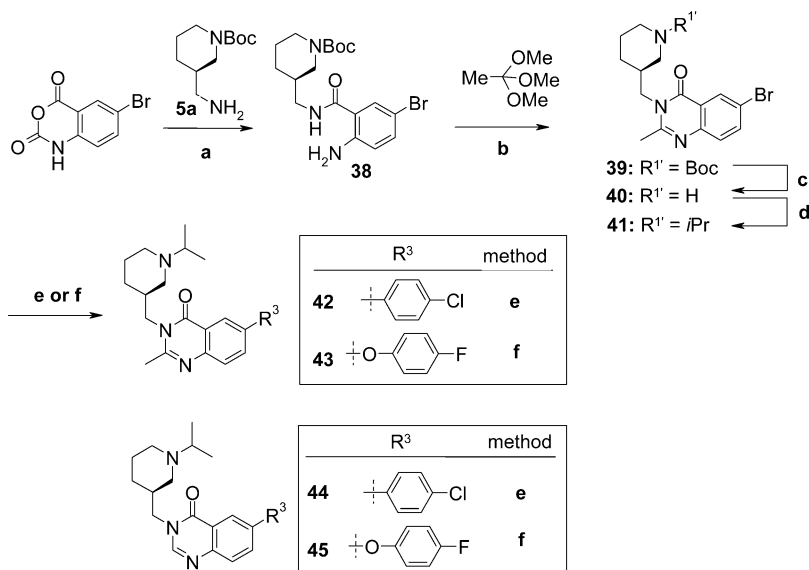
While alkoxy derivatives **30** and **31** were derived from available anthranilic acid starting materials, phenoxy analogues **34** and **35** were formed using the Ullmann coupling reaction (Scheme 6).[30] The (*S*)-phenoxy analogues **36** and **37** were synthesized in an analogous manner (Scheme 6).

As described in Scheme 7, a more concise method was used to build the quinazolinone ring carrying small substituents (H, CH_3) at the 2-position (R^2).[31,32] Coupling of a phenyl or phenoxy group at the 6-position of the quinazolinone ring was performed as outlined in Schemes 1 and 6.

Results and Discussion

In Vitro SAR Studies. Affinity for GHS-R1a was determined using a [^{125}I]ghrelin displacement assay [scintillation proximity assay (SPA) format] employing membranes prepared from a human embryonic kidney cell line (HEK293F) overexpressing recombinant GHS-R1a. The functional activity of test compounds was assessed by measuring GTPγS binding to membranes likewise prepared from HEK293F cells overexpressing recombinant GHS-R1a.

As we sought to replace the *N*-methyl-*N*-butyl moiety of lead compound **2** due to its metabolic lability, we started our SAR investigations at the 6- and 7-positions of the quinazolinone ring (R^3 and R^4). Initial SAR studies had suggested as preferred R^1 (3-position of quinazolinone ring) an *N*-ethyl- or *N*-isopropyl-substituted methylpiperidine moiety and as preferred R^2 (2-position of quinazolinone ring) an ortho-substituted phenyl group. As can be seen from Table 1, a bulky group at the

Scheme 6[a,b]

36: $R^2 =$
37: $R^2 = iPr$

[a] Reagents and conditions: (a) Toluene, reflux; ethylene glycol, LiOH, 135 °C, 48%. (b) 4-Fluorophenol, CuCl, TMHD, Cs_2CO_3, NMP; 46%. (c) TFA, CH_2Cl_2, 78%. (d) 2-Iodopropane, K_2CO_3, CH_3CN, 70 °C, 86%. [b] Compounds **37** and **38** were synthesized in an analogous fashion using homochiral piperidine building block **5a**.

Scheme 7[a]

[a] Reagents and conditions: (a) K_2CO_3, THF, 70 °C, 86%. (b) 140 °C. (c) TFA, CH_2Cl_2. (d) 2-Iodopropane, K_2CO_3, CH_3CN, 70 °C, 80% (three steps). (e) 4-Chlorophenylboronic acid, Cs_2CO_3, $PdCl_2(dppf)$, DME, H_2O, 60 °C. (f) 4-Fluorophenol, Cs_2CO_3, CuCl, TMHD, NMP, microwave, 205 °C.

Table 1. SAR Investigation at the 6- and 7-Positions of the Quinazolinone Core[a]

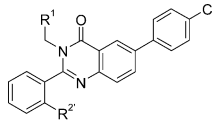| No.	R[1']	R[2']	R[3]	R[4]	GHS-R binding K_i [nM]	GHS-R antagonism Kb_{app} [nM]	GHS-R agonism E/E_{max} [%]	Rat PK, C_{max} [μM][b]
29	*i*Pr	Me	H	H	1,200	n.d.	n.d.	n.d.
30	Et	OMe	OMe	H	910	n.d.	n.d.	n.d.
31	Et	Me	OCF_3	H	24	45	4	0.23
34	H	Me	⊹O-⟨⟩-F	H	0.9	n.d.	92[c]	0.04
35	*i*Pr	Me	⊹O-⟨⟩-F	H	0.47	0.97	23	0.31
7	H	Me	⊹-⟨⟩-Cl	H	7.0	13	12	0.02
8	Et	Me	⊹-⟨⟩-Cl	H	1.8	3.2	12	0.12
28	Et	OMe	H	⊹-⟨⟩-Cl	> 10,000	n.d.	n.d.	n.d.

[a] Reported in vitro values are an average of at least two replicates. [b] Pharmacokinetic screening study in Wistar rat; compounds were orally administered at 3 mg/kg in PEG400/methanesulfonic acid (80:20) vehicle. [c] GHS-R agonism EC_{50} = 6.5 nM.
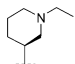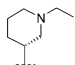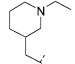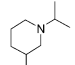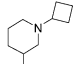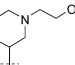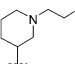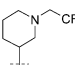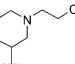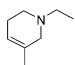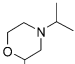
6-position (R^3) is essential for activity. While phenoxy substituents confer slightly higher binding affinities, the more rigid phenyl analogues bear less potential for undesired partial agonism. Interestingly, even the unsubstituted piperidine analogue in the phenyl series (**7**) is an antagonist, which is opposite from the corresponding phenoxy analogue **34** as well as the amino-substituted screening hit **1**. Following this observation, we concentrated further SAR efforts on compounds carrying phenyl groups at the 6-position.

Plasma exposure (3 mg/kg p.o., rat) of compounds shown in Table 1 was improved over the initial lead compound **2** (C_{max}

< 20 nM at 10 mg/kg p.o., rat), indicating that the metabolic instability of the *N*-methyl-*N*-butyl moiety of **2** had in fact contributed to its weak exposure. We also determined the oral bioavailability of the HCl salt of compound **8** in rat and found it to be moderate (29%) (p.o. study conducted at 3 mg/kg, i.v. study conducted at 1 mg/kg).

Among the two enantiomers of compound **8**, the (*S*)-stereoisomer **24** was found to be significantly more potent than the (*R*)-isomer **25** (Table 2). This enantiospecific activity appeared to be general for this class, also with substantially modified analogues (see the Supporting Information). Extension

Table 2. SAR Investigations at the Piperidine Ring[a]

No.	R^1	R$^{2'}$	GHS-R binding Ki [nM]	GHS-R antagonism Kb$_{app}$ [nM]	GHS-R agonism E/E$_{max}$ [%]	pKa [b]	Rat PK, Cmax [μM][c]
24		Me	1.7	2.8	0	9.6	0.12
25		Me	71	250	10	9.6	n.d.[d]
15		OMe	> 10,000	n.d.	n.d.	9.8	n.d.
9		Me	1.8	0.9	-20	10.0	0.15
10		Me	2.5	2.7	-20	9.6	0.22
11		Me	4.0	6.4	-20	8.6	0.14
12		Me	16	14	-9	8.0	0.10
13		Me	2,000	n.d.	n.d.	4.3	0.17
14		Me	250	n.d.	n.d.	8.2	n.d.
18		Me	26	36	-18	8.7	0.03
23		Me	190	n.d.	n.d.	7.7	n.d.

[a] Reported in vitro values are an average of at least two replicates. [b] Calculated using ACD software.[34] [c] Pharmacokinetic screening study in rat; compounds were orally administered at 3 mg/kg in PEG400/methanesulfonic acid (80:20) vehicle. [d] Not determined.

of the piperidine linker by one CH$_2$ unit (**15**) resulted in loss of activity. Particular attention was laid on studying the dependence between activity and pK$_a$, since the pK$_a$ of alkyl-substituted piperidine analogues was very high (∼10), potentially compromising pharmacokinetic properties.[33] Modulation of the pK$_a$ was achieved by introducing electronegative atoms at the ring itself as well as at its periphery, and selected compounds derived from these efforts are shown in Table 2. While pK$_a$ values down to at least 8 were tolerated without substantial loss of GHS-R1a affinity, none of these changes had any apparent effect on plasma exposure in rats.

As a potential measure for improving DMPK properties, we took an active effort to reduce lipophilicity.[35] This pursuit led us to the 2-position of the quinazolinone ring. As shown in Table 3, decreasing the size of the R^2 substituent gradually weakened activity, but the effect was relatively small, particularly for the series with R^3 = phenoxy where even the unsubstituted analogue **45** (R^2 = H) still possesses ghrelin binding affinity of <50 nM. Although activity losses arose from decreasing the size of the R^2 group, clear benefits resulted for other drug property features, such as solubility and selectivity. For example, 2-phenyl analogue **24** (R^3 = phenyl) displayed high binding affinity to

the 5-HT$_{2c}$ receptor and phenyl analogue **36** (R^3 = phenoxy) was a potent CYP2D6 inhibitor, while analogues with smaller groups were devoid of such selectivity issues and furthermore showed superior aqueous solubility. Interestingly, compounds with alkyl groups larger than ethyl on the piperidine nitrogen in the R1 position (compounds **9**−**12**) showed a trend toward inverse agonism. A similar trend toward inverse agonsim was also seen in the alkylated dehydropiperidine-derived compound **18**.[36]

In Vivo Studies. Further investigations were carried out on the 2-isopropyl-6-phenyl derivative **26** and the 2-methyl-6-phenoxy derivative **43**. Both compounds are potent and selective[38] GHS-R1a antagonists with K$_b$ values of 14 and 11 nM, respectively. Key pharmacokinetic data of **26** and **43** in rat are shown in Table 4. Both compounds display high bioavailability, moderate clearance, and very high volumes of distribution. While a high volume of distribution was a general feature of this compound class, clearance and bioavailability of **26** and **43** were significantly improved over first generation analogues.

There is compelling evidence that ghrelin plays a critical role in modulating body weight through the control of food intake

Table 3. SAR Investigations at the 2-Position of the Quinazolinone Core[a]
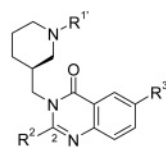
No.	R1'	R2	R3	GHS-R binding Ki [nM]	GHS-R antagonism Kb$_{app}$ [nM]	GHS-R agonism E/E$_{max}$ [%]
24	Et	(2-methylphenyl)	(phenyl)–Cl	1.7	2.8	0
26	iPr	iPr	(phenyl)–F	39	14	15
27	iPr	iPr	(phenyl)–Cl	45	77	0
45	iPr	Me	(phenyl)–Cl	110	430	0
44	iPr	H	(phenyl)–Cl	440	n.d.	n.d.
36	iPr	(2-methylphenyl)	O–(phenyl)–F	0.86	0.19	22
37	iPr	iPr	O–(phenyl)–F	4.0	7.6	-5
43	iPr	Me	O–(phenyl)–F	17	11	11
45	iPr	H	O–(phenyl)–F	18	45	2

No.	cLogP[b]	Aq. solubility (pH 7.2) [μM][c]	5-HT$_{2c}$ Ki [nM][d]	CYP2D6 inhibition IC$_{50}$ [μM][e]	Rat PK, C$_{max}$ [μM][f]
24	7.2	80	120 nM [g]	6.1	0.12
26	6.1	280	> 1 μM	6.9	0.15
27	6.6	60	> 1 μM	6.3	0.29
45	5.7	125	> 1 μM	9.6	n.d.
44	5.2	n.d.	> 1 μM	> 100	0.20
36	7.1	250	> 1 μM	0.04	0.09
37	6.3	100	> 1 μM	7.2	0.21
43	5.4	500	> 1 μM	13	0.22
45	4.9	450	> 1 μM	21	n.d.

[a] See the corresponding footnote in Table 1. [b] Calculated using Daylight software.[37] [c] Kinetic solubility determined by HPLC; buffered aqueous test solution contained 1% DMSO. [d] Assay information given in the Experimental Section. [e] Determined using CYPD26 supersomes and the fluorescent substrate 3-[2-(N,N-diethyl-N-methylamino)ethyl]-7-methoxy-4-methylcoumarin (AMMC). [f] Pharmacokinetic screening study in Wistar rat; compounds were orally administered at 3 mg/kg in PEG400/methanesulfonic acid (80:20) vehicle. [g] Compound was found to be a 5-HT$_{2c}$ antagonist.

and/or regulation of fuel substrate efficiency. We therefore tested the effects of the GHS-R1a antagonists **26** and **43** on food intake in the mouse fasted−refed model. As shown in Figure 1, upon oral administration at a dose of 30 mg/kg, both compounds caused significant suppression of food intake throughout the period from 1 to 24 h, with **26** being the more efficacious compound.

Following the food intake studies, we examined the effects of **26** and **43** on body weight in diet-induced obese (DIO) mice. Over a period of 9 days, compounds were orally administered once daily at doses of 3, 10, and 30 mg/kg (Figure 2). While compound **26** lowered body weight at the 10 mg/kg dose, compound **43**, consistent with a weaker effect in the food intake study, was efficacious only at the highest dose of 30 mg/kg,

Table 4. Pharmacokinetic Profile of Compounds **26** and **43** in Rat[a]

	compound			
	26		**43**	
route	i.v.	p.o.	i.v.	p.o.
dose (mg/kg)	0.7	3	1	3
AUC_{0-t} (mg h/L)	0.58	1.7	0.50	1.3
C_{max} (mg/L)	0.10	0.07	0.11	0.08
$T_{1/2}$ (h)	16		19	
CL (L/kg h)	1.2		1.9	
V_{ss} (L/kg)	18.8		19.2	
F (%)		69		85

[a] The pharmacokinetic parameter estimates of compound **26** and **43** were evaluated in male Wistar rats following single-dose i.v. administration at ~1 mg/kg and oral administration at 3 mg/kg. Test compounds were freshly prepared before dosing in rat plasma (2% DMSO) as a solution for i.v. administration and in PEG400/methanesulfonic acid 10 mM (80:20, v/v) as a solution for oral administration.
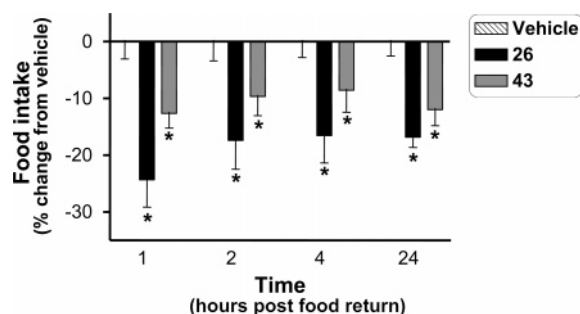

Figure 1. Acute effects of compounds **26** and **43** on food intake in the mouse fasted−refed model (lean C57 black mice). Both compounds were orally administered at a dose of 30 mg/kg (vehicle, PEG400/water 50:50).
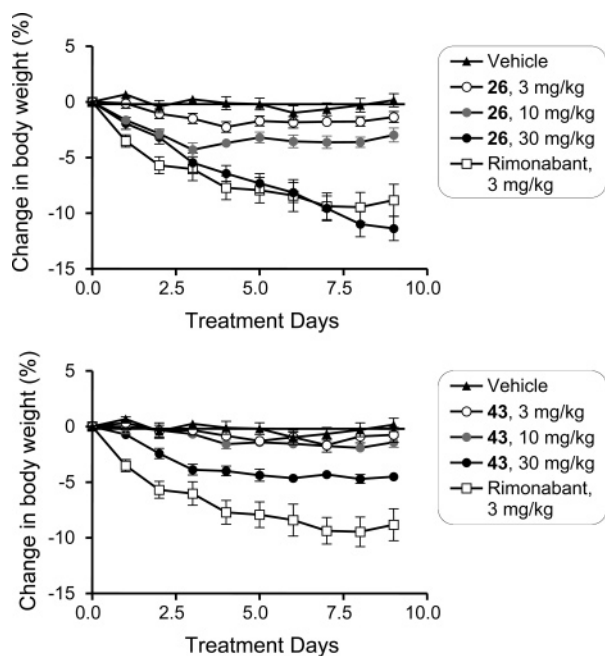

Figure 2. Effect of compounds **26** and **43** on body weight in DIO mice. The CB1 antagonist rimonabant was used as a positive control. Compounds were administered by oral gavage once daily for 9 days (vehicle, PEG400/water 50:50).

producing a 5% decrease in body weight. The effect of compound **26** at the 30 mg/kg dose, on the other hand, was very strong, and progression of body weight loss was comparable to the effect achieved with the CB1 antagonist rimonabant, 5-(4-chlorophenyl)-1-(2,4-dichlorophenyl)-4-methyl-N-(piperidin-1-yl)-1H-pyrazole-3-carboxamide, an anti-obesity drug cur-

rently under evaluation by the FDA.[39] This, to the best of our knowledge, constitutes the first reported case of an orally administered GHS-R1a antagonist that promotes chronic body weight loss in animals. One of the concerns that has been raised about the utility of GHS-R1a antagonists for treatment of obesity is that in obese patients ghrelin levels are significantly reduced,[40] with parallel observations made for obese rodents.[41] Our data show that, despite the decreased ghrelin levels in DIO mice, the ghrelin tone is still sufficient to allow antagonists to be effective.

A possible explanation for the difference in efficacy between compounds **26** and **43** despite comparable in vitro activity and plasma exposure was a difference in brain exposure. Pharmacokinetic studies on both compounds and other quinazolinone derivatives in fact revealed that the effect on food intake in mice is dependent on the drug levels detected in the brain (Table 5). Thus, compound **26**, a highly brain-exposed compound, effectively lowered food intake in a mouse fasted−refed model, while the lesser brain-exposed compound **43** was weaker in this regard. Consistent with these findings, compound **46**,[42] a potent ghrelin antagonist with high plasma exposure in mice, but nondetectable brain levels, was entirely inactive in the food intake model. These results are in agreement with data by others showing that ghrelin antagonists with an effect on food intake are exposed in the brain.[43] Thus, given that the effects of **26** and **43** on body weight are driven by suppression of food intake, the difference in brain exposure could contribute to the difference in efficacy in the DIO mouse model. Further support for this hypothesis would require detailed measurements of free brain concentrations at various time points throughout the chronic study and examination of compounds with greater differences in brain exposure.

The different degree of brain exposure of the compounds shown in Table 4 can partly be rationalized by differences in their polar surface area and number of rotational bonds, two important physicochemical determinants for blood−brain barrier permeability (Table 5).[44]

Recent studies conducted by us and others have demonstrated that ghrelin suppresses insulin secretion and that this effect is mediated through GHS-R1a.[12,14,46] Consequently, GHS-R1a antagonism has been put forth as a potential approach for improving glucose homeostasis and treatment of type 2 diabetes. The quinazolinone derivatives **26** and **43** are potent and selective GHS-R1a antagonists with favorable pharmacokinetic properties and, hence, were well-suited small-molecule proof-of-concept tools for this hypothesis.

As first indication of the validity of the hypothesis, we demonstrated that GHS-R1a antagonists from the quinazolinone class block the inhibitory effect of ghrelin on insulin secretion in vitro.[47] This finding is in agreement with data obtained with peptidic GHS-R1a antagonists.[12] Encouraged by these results, we investigated the effects of our compounds on glucose homeostasis in vivo, using an IP glucose tolerance test (IPGTT) in rats (Figure 3). Upon glucose administration, 10 mg/kg oral doses of compound **26** produced a 20% and compound **43** a 23% decrease in the glucose excursion relative to the vehicle-treated animals. This effect was similar in magnitude to the effect of parenterally administered ANC7-PEG, a peptide dual-acting GLP-1 agonist and glucagon antagonist with a strong glucose-lowering effect in glucose tolerance models.[48] In another study, we could demonstrate that the underlying mechanism of promoting a decrease in glucose excursion is in fact increased insulin secretion.[47] To evaluate if GHS-R1a antagonists are prone to causing hypoglycemia, the effect of superefficacious

Table 5. Effect of GHS-R1a Antagonists with Differing CNS Exposures on Food Intake in the Fasted−Refed Model

				GHS-R1a		Mouse PK, 30 mg/kg p.o. [a]		Change in food intake at 30 mg/kg [b]
No.	$R^{1'}$	R^2	R^3	K_i [nM]	$Kb_{app.}$ [nM]	C_{max} [μM]	Brain level (% of plasma conc.)	
26	*i*Pr	*i*Pr	(phenyl)—F	27	26	0.8	76	-17%
24	Et	(tolyl)	(phenyl)—Cl	2	3	2.2	22	-17%
43	*i*Pr	Me	O—(phenyl)—F	17	11	3.4	19	-12%
36	*i*Pr	(tolyl)	O—(phenyl)—F	0.8	0.2	3.1	1	-7%
46[c]	*i*Pr	HO(ethoxy)(phenyl)F	O—(phenyl)—F	2	2	5.7	<0.001	+1%

No.	PSA [Å^2][d]	Σ rotational bonds
26	36	5
24	36	5
43	45	5
36	45	6
46	77	10

[a] Plasma and brain exposure were tested 5 h after compound administration; studies were conducted in C57 lean black mice. [b] Twenty-four hours of cumulative food intake at compound doses of 30 mg/kg in a mouse fasted−refed model; studies were conducted in C57 lean black mice. [c] Compound **46** was a racemate. [d] Topological PSA (TPSA) calculated according to Ertl et al.[45]

Table 6. Effect of GHS-R1a Antagonists with Differing CNS Exposures on Glucose Excursion (AUC) in the Rat IPGTT Model

	mouse PK, 3 mg/kg p.o.		
no.	C_{max} (μM)	brain level (% of plasma concn)	change in blood glucose at 10 mg/kg[a]
26	0.8	76	−20%
24	2.2	22	−13%
43	3.4	19	−23%
36	3.1	1	−19%
46[b]	5.7	<0.001	n.d.

[a] Decrease in blood glucose AUC relative to vehicle-treated group in the rat IPGTT model. [b] Compound **46** was a racemate; this compound was not tested in the IPGTT model because of insufficient plasma exposure in rat.

compound doses on blood glucose levels in fasted animals was examined, and no physiologically relevant changes in blood glucose were observed.[47] These data represent the first reported case of an orally administered selective ghrelin antagonist with a beneficial effect on glucose homeostasis.

Interestingly, compound **36** (Table 5), which displayed poor (1%) mouse brain exposure and had a modest effect on feeding, was found to be fully active in the rat IPGTT model. This observation is consistent with the hypothesis that the effects of ghrelin and GHS-R1a antagonists on glucose homeostasis are peripherally driven through a direct effect on pancreatic islets.[47] One caveat with this interpretation is that brain exposure was measured in mice and that the IPGTT was conducted in rats.

Summary

Piperidine-substituted quinazolinone derivatives were identified as a new class of small-molecule GHS-R1a modulators. Starting from a GHS-R1a agonist with poor oral bioavailability, structural optimization led to potent, selective, and orally bioavailable antagonists. A key SAR finding was the identification of phenyl or phenoxy groups as optimal substituents at the
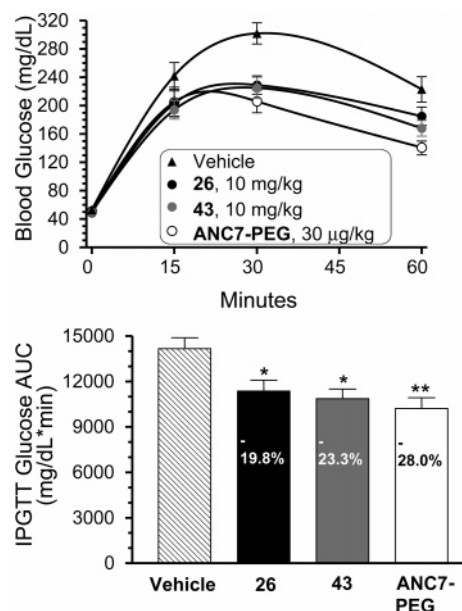
Figure 3. Effect of compounds **26** and **43** in a rat IPGTT at 10 mg/kg p.o. (vehicle, PEG400/10 mM methanesulfonic acid 80:20). Five hours after compound p.o. administration, a 2 g/kg glucose challenge was administered by intraperitoneal injection. A group treated with the peptide ANC7-PEG[48] was used as a positive control (i.p. administration). Relative to vehicle, compound **26** produced a 20% and compound **43** a 23% decrease in glucose AUC over the course of the experiment.

6-position of the quinazolinone core. At the slight sacrifice of potency, but beneficial for selectivity and DMPK properties, phenyl groups at the 2-position were then replaced by small alkyl substituents. Two compounds emerging from this effort, **26** and **43**, were found to show high bioavailability in pharmacokinetic studies in rats and were selected for in vivo efficacy evaluation.

Ghrelin is known to play a critical role in modulating body weight mainly through control of food intake. In a fasted−refed model in mice, both **26** and **43** caused a significant suppression of food intake. An independent in vivo study in DIO mice showed that both compounds promoted weight loss; in fact, **26** demonstrated at the highest dose comparable efficacy to the anti-obesity drug rimonabant, a CB1 antagonist.

On the basis of numerous literature reports, GHS-R1a antagonism has been proposed as a concept for stimulating insulin secretion with potential use in the treatment of type 2 diabetes. Therefore, compounds **26** and **43** were tested in a glucose tolerance test in rats and, as well as other structural analogues in this class, produced a decrease in glucose excursion to a similar degree as a highly efficacious benchmark insulin secretagogue. In vitro and in vivo studies demonstrated that the underlying effect was compound-mediated glucose-dependent stimulation of insulin secretion through action on GHS-R1a.

The compounds presented in this account, piperidine-substituted quinazolinone derivatives, represent the first reported examples of orally available GHS-R1a antagonists that promote chronic body weight loss and improve glucose homeostasis in animal models. These results suggest GHS-R1a antagonism as an attractive approach for treating metabolic disorders through improving the diabetic phenotype while targeting obesity as the root cause of the disease.[47]

Experimental Section

In Vitro Assays. GHS-R1a Pharmacology. The affinity for GHS-R1a was determined using a radioligand binding assay. Test compound and 50 pM [^{125}I]ghrelin were mixed in buffer (25 mM HEPES, pH 7.4, 5 mM magnesium chloride, 1 mM calcium chloride, 1 mM EDTA, and 0.1% BSA). A suspension of membrane from HEK293S cells overexpressing ovine GHS-R1a was preincubated for 30 min with 5 mg/mL wheatgerm agglutinin SPA beads and then added to the wells containing test compound and [^{125}I]-ghrelin. Nonspecific binding is defined using 1 μM ghrelin peptide. Following a 2 h incubation at room temperature, the amount of [^{125}I]ghrelin bound to the membranes was measured.

The functional activity of the program compounds was measured using GTPγS binding to membranes prepared from HEK293F cells overexpressing recombinant GHS-R1a. GHS-R1a agonism was deduced from stimulation of GTPγS binding above basal levels by compound. In this assay, partial agonists were defined as compounds that stimulated GTPγS binding 20−85% relative to ghrelin (defined as 100%), while full agonists were defined as compounds that stimulated GTPγS binding >85% relative to ghrelin. Compounds that failed to show agonist or partial agonist activities were evaluated for their ability to serve as antagonists. Ghrelin dose−response curves were performed in the absence and presence of a fixed concentration of the putative antagonist. The membrane from HEK293S cells overexpressing GHS-R1 was mixed with test compound and/or ghrelin in buffer (25 mM HEPES, 50 mM sodium chloride, 10 mM magnesium chloride, 1 μM GDP, and 0.1% BSA, pH 7.4) and 200 pM [^{35}S]GTPγS. After a 60 min room temperature incubation, bound and free [^{35}S]GTPγSs were separated by filtering through GF/B membranes. After multiple washes, the amount of [^{35}S]GTPγS on the filtered membranes was determined. Nonspecific binding was defined in the presence of 10 μM GTPγS.

5-HT$_{2c}$ Radioligand Binding Assay. The affinity for the 5-HT$_{2c}$ receptor was determined using a radioligand binding assay. Test compound and 250 pM (±)-1-(2,5-dimethoxy-4-[^{125}I]iodophenyl)-2-aminopropane ([^{125}I]DIO) were mixed in buffer (50 mM Tris, pH 7.4, 10 mM magnesium chloride, 10 μM paragyline, 0.1% sodium ascorbate, 0.5 mM EDTA, and 0.1% BSA). A suspension of membrane from cells stably overexpressing the 5-HT$_{2c}$ receptor and wheatgerm agglutinin SPA beads (200 μg) was added to the wells containing test compound and [^{125}I]DIO. Nonspecific binding

was defined using 10 μM 5-HT. Following a 1 h incubation at room temperature, the amount of [^{125}I]DIO bound to the membranes was measured.

In Vivo Assays. Glucose Tolerance Tests in Rats. Male Wistar rats were fasted overnight (16−18 h) and then given ghrelin antagonist or vehicle (PEG400/10 mM MSA 80:20) by oral gavage. Five hours after dosing, the fasting blood glucose level was measured from tail-tip blood using a Glucometer (Bayer Corp., Mishawaka, IN), and the animals were given 2 g/kg of glucose by either intraperitoneal injection (IPGTT) or by oral gavage (OGTT). Blood glucose was measured again after 15, 30, and 60 min for the IPGTT. Additional blood glucose measurements were made after 90 and 120 min for the OGTT or after 90 min when an IPGTT was performed with DIO rats. The area under the glucose curve (AUC) from 0 to 60, 0 to 90, or 0 to 120 min was calculated using the trapezoidal method, and the effect of the compound on the AUC was expressed as a percentage of the AUC for the vehicle-treated group. When insulin levels were measured, 0.05 mL of blood was collected in a capillary tube at the same time periods as described. Insulin was determined using an enzyme-linked immunosorbent assay (Alpco Diagnostics, Windham, NH).

DIO Mouse Model. Male C57BL/6 mice were fed a high-fat diet (containing 45% calories from fat) for 16 weeks before the start of the studies. The animals included in the studies had an average body weight greater than 4 standard deviations of the mean body weight of mice that were fed a standard low-fat diet (5% calories from fat). GHS-R1a antagonists, rimonabant, or vehicle was administered orally approximately 0.5−1.0 h before the feeding phase (dark cycle). Daily body weight and food intake were recorded during treatment. Fat and lean mass were measured in each animal at the start and end of the studies using NMR imaging. Pair feeding was performed by measuring the 24 h food intake of compound-treated mice each day and limiting food consumption to that amount in a group of vehicle-treated mice.

Mouse Fasted Refed Model. Male C57BL/6 mice were fasted overnight and dosed the following day, 1 h before refeeding. The cumulative food intake was recorded for a period of 24 h after food return.

General Chemistry. Purchased reagents and anhydrous solvents were used as received. Air and moisture sensitive liquids and solutions were transferred via syringe or cannula and introduced into reaction vessels through rubber septa. Column chromatography was performed on a Biotage system using 32−63 μm, 60 Å, silica gel prepacked cartridges.

Purification using preparative reversed-phase HPLC chromatography was accomplished using a Gilson 215 system, using a YMC Pro-C18 AS-342 (150 mm × 20 mm i.d.) column and 1 mL/min flow rate. Typically, the mobile phase used was a mixture of H$_2$O (A) and MeCN (B). The water could be mixed or not with 0.1% TFA. A typical gradient was as follows: 0.5 min, 90% A and 10% B; 11.0 min, 0% A and 100% B.

Chiral analytical HPLC experiments were performed using one of the two following methods using a Varian Pro Star 1200. Method A: Chiracel AD column, 4.6 mm (i.d.) × 250 mm; mobile phase: A, 0.1% TFA in hexanes; B, 0.1% TFA in *i*-PrOH; isocratic: 95% A (5% B), 20 min; flow rate, 1.5 mL/min; and UV detection, 284 nm. Method B: Chiracel AD column, 4.6 mm (i.d.) × 250 mm; mobile phase: A, 0.1% TFA in hexanes; B, 0.1% TFA in *i*-PrOH; isocratic: 95% A (5% B), 25 min; flow rate, 1.0 mL/min; and UV detection, 284 nm.

Electron impact mass spectra (EI-MS or GC-MS) were obtained with a Hewlett-Packard 5989A mass spectrometer equipped with a Hewlett-Packard 5890 Gas Chromatograph with a J & W DB-5 column (0.25 μM coating; 30 m × 0.25 mm). The ion source was maintained at 250 °C, and spectra were scanned from 50 to 800 amu at 2 s per scan.

Two different methods were used to obtain HPLC−electrospray mass spectra (HPLC-ES MS). HPLC-MS method 1: An Agilent 1100 HPLC system was equipped with an Agilent 1100 autosampler, quaternary pump, and a diode array. The HPLC column used

was a Waters Sunfire C-18 column (2.1 mm × 30 mm, 3.5 μM). The HPLC eluent was directly coupled with a 1:4 split to a Finnigan LTQ ion trap mass spectrometer with electrospray ionization. Spectra were scanned from 50 to 800 amu using a variable ion time according to the number of ions in the source using positive ion mode. The eluents were A, water with 0.1% formic acid, and B, acetonitrile with 0.1% formic acid. Gradient elution from 10 to 90% B over 3.0 min at a flow rate of 1.0 mL/min was used with an initial hold of 2.0 min and a final hold at 95% B of 1.0 min. The total run time was 8.0 min.

HPLC-MS method 2: An Agilent 1100 HPLC system was equipped with an Agilent 1100 autosampler, quaternary pump, and a variable wavelength detector set at 254 nm. The HPLC column used was a Waters Sunfire C-18 column (2.1 mm × 30 mm, 3.5 μM). The HPLC eluent was directly coupled without splitting to a Finnigan LCQ DECA ion trap mass spectrometer with electrospray ionization. Spectra were scanned from 140 to 1200 amu using a variable ion time according to the number of ions in the source using positive ion mode. The eluents were A, 2% acetonitrile in water with 0.02% TFA, and B, 2% water in acetonitrile with 0.02% TFA. Gradient elution from 10 to 90% B over 3.0 min at a flow rate of 1.0 mL/min was used with an initial hold of 1.0 min and a final hold at 95% B of 1.0 min. The total run time was 7.0 min. For consistency in characterization data, the retention time (RT) is reported in min at the apex of the peak as detected by the UV−vis detector set at 254 nm.

^{1}H NMR spectroscopy was performed on 300 or 400 MHz Varian Mercury-plus as well as Bruker DRX500 spectrometers. The samples were dissolved in deuterated solvents and transferred to 5 mm i.d. Wilmad NMR tubes. The spectra were acquired at 293 K. The chemical shifts were recorded on the ppm scale and were referenced to the appropriate residual solvent signals, such as 2.49 ppm for DMSO-d_6, 1.93 ppm for CD_3CN, 3.30 ppm for CD_3OD, 5.32 ppm for CD_2Cl_2, and 7.26 ppm for $CDCl_3$.

Synthetic Procedures and Compound Characterization. 6-Bromo-2-(2-methylphenyl)-4H-3,1-benzoxazin-4-one (3). *o*-Toluoyl chloride (10.0 g, 64.7 mmol) was added slowly into a mixture of 2-amino-5-bromobenzoic acid (12.7 g, 58.8 mmol) and triethylamine (24.6 mL, 176.4 mmol) in CH_2Cl_2 (120 mL) at 0 °C. The reaction mixture was stirred at rt for 14 h. Half of the CH_2Cl_2 was removed under reduced pressure, acetic anhydride (50 mL) was added, and the mixture was heated at 50 °C for 2 h. The reaction mixture was cooled to rt, quenched by slow addition of ice water, and diluted with CH_2Cl_2. The layers were separated, and the organic layer was washed with $NaHCO_3$ and brine and dried over Na_2SO_4. After it was concentrated under reduced pressure, the crude product was treated with ethanol and stirred for 10 min. The solid was filtered and washed with additional ethanol. It was then dried in a vacuum oven at 50 °C for 3 h to give 11.5 g (62%) of the product. LC-MS method 2: *m/z* 316.3 (MH⁺); RT (min) 3.71.

6-(4-Chloro-phenyl)-2-methylphenyl-4H-3,1-benzoxazin-4-one (4). Under an argon atmosphere, 6-bromo-2-(2-methylphenyl)-4H-3,1-benzoxazin-4-one (3) (7.4 g, 23.4 mmol), 4-chlorophenylboronic acid (5.5 g, 35.1 mmol), K_2CO_3 (19.4 g, 140.4 mmol), and $PdCl_2(dppf)$ were combined in a mixture of toluene (40 mL), 1,4-dioxane (10 mL), and water (8 mL). The reaction mixture was stirred for 30 min at 50 °C and then cooled to rt, filtered, and concentrated under reduced pressure. Silica gel flash chromatography using a gradient of hexane → EtOAc/hexane 1:7 yielded the product as a light yellow solid (5.9 g, 73%).

***tert*-Butyl 3-{[6-(4-Chlorophenyl)-2-(2-methylphenyl)-4-oxoquinazolin-3(4H)-yl]methyl}piperidine-1-carboxylate (6).** *tert*-Butyl 3-(aminomethyl)piperidine-1-carboxylate (600 mg, 2.80 mmol) in toluene (10 mL) was added to 6-(4-chlorophenyl)-2-(2-methylphenyl)-4H-3,1-benzoxazin-4-one (811 mg, 2.33 mmol), and the solution was stirred at reflux for 16 h under a nitrogen atmosphere. The mixture was concentrated under reduced pressure and passed through a silica gel plug (100% EtOAc). This gave the intermediate product as a yellow oil, which was used for next step without further purification.

The above intermediate (746 mg, 1.33 mmol) was added to a dry round-bottom flask followed by ethylene glycol (10 mL) and LiOH (112 m g, 2.65 mmol). The resulting mixture was stirred at 135 °C for 16 h. The reaction mixture was diluted with CH_2Cl_2 and water. The aqueous mixture was extracted with CH_2Cl_2 (20 mL × 2), and the organic solvent was removed under reduced pressure. The crude product was then purified by silica gel flash chromatography with 10−50% ethyl acetate in hexanes to give the product (803 mg, 63%). LC-MS method 2: *m/z* 544.6 (MH⁺); RT (min) 4.38.

6-(4-Chlorophenyl)-2-(2-methylphenyl)-3-(piperidin-3-ylmethyl)-quinazolin-4(3H)-one (7). To a solution of *tert*-butyl 3-{[6-(4-chlorophenyl)-2-(2-methylphenyl)-4-oxoquinazolin-3(4H)-yl]methyl}-piperidine-1-carboxylate (450 mg, 0.83 mmol) in CH_2Cl_2 (8 mL) was added TFA (4 mL), and the reaction mixture was stirred at rt for 3 h. The solvents were removed, and the crude product was redissolved in ethyl acetate. The organic layer was washed with saturated aqueous $NaHCO_3$ and brine and dried over Na_2SO_4. Filtration and removal of the solvent under reduced pressure gave the product (302 mg, 82%). ^{1}H NMR (400 MHz, methanol-d_4): δ ppm 8.47 (d, *J* = 2.14 Hz, 1 H), 8.12 (dd, *J* = 8.48, 1.66 Hz, 1 H), 7.71−7.76 (m, 3 H), 7.50 (t, *J* = 7.99 Hz, 4 H), 7.39−7.41 (m, 2 H), 4.08−4.23 (dd, *J* = 13.74, 7.89 Hz, 1 H), 3.46−3.66 (dd, *J* = 13.64, 7.99 Hz, 1 H), 2.94 (s, 1 H), 2.90 (d, *J* = 7.21 Hz, 1 H), 2.44−2.55 (m, 1 H), 2.17−2.28 (m, 3 H), 1.88 (s, 1 H), 1.85 (d, *J* = 3.51 Hz, 1 H), 1.56−1.67 (m, 2 H), 1.33−1.43 (m, 2 H), 1.00−1.11 (m, *J* = 11.50, 11.50, 11.21, 8.48 Hz, 1 H). LC-MS method 1: *m/z* 444.3 (MH⁺); RT (min) 4.25. LC-MS method 2: *m/z* 444.2 (MH⁺); RT (min) 2.84.

6-(4-Chlorophenyl)-3-[(-1-ethylpiperidin-3-yl)methyl]-2-(2-methylphenyl)quinazolin-4(3H)-one (8). To a solution of **7** (416 mg, 0.94 mmol) in THF (20 mL) was added acetaldehyde (0.06 mL, 1.03 mmol) at 0 °C, followed by rapid addition of AcOH (0.06 mL, 1.12 mmol) and sodium triacetoxyborohydride (278 mg, 1.31 mmol). The reaction mixture was stirred under nitrogen atmosphere at rt for 4 h. Saturated aqueous $NaHCO_3$ solution was added, and the mixture was stirred at rt for 15 min. The mixture was diluted with CH_2Cl_2 (50 mL), and the organic layer was separated, washed with brine, dried over Na_2SO_4, filtered, and concentrated under reduced pressure. The crude product was purified by HPLC with 10−80% CH_3CN in water (0.1% TFA) to give the product (306 mg, 69%) as a light yellow oil. ^{1}H NMR (400 MHz, methanol-d_4): δ ppm 8.49 (d, *J* = 1.57 Hz, 1 H), 8.13 (dd, *J* = 8.41, 2.15 Hz, 1 H), 7.75 (dd, *J* = 8.31, 2.05 Hz, 3 H), 7.47−7.53 (m, 4 H), 7.38−7.44 (m, 2 H), 4.15−4.21 (m, 1 H), 3.52−3.62 (m, 1 H), 2.84 (t, *J* = 9.49 Hz, 1 H), 2.76 (d, *J* = 10.96 Hz, 1 H), 2.32−2.41 (m, 2 H), 2.28 (d, *J* = 4.89 Hz, 3 H), 1.89−1.99 (m, 1 H), 1.80−1.89 (m, 1 H), 1.53−1.64 (m, 2 H), 1.41−1.47 (m, 1 H), 1.32−1.39 (m, 1 H), 1.02 (dt, *J* = 9.78, 7.24 Hz, 3 H), 0.89−0.96 (m, 1 H). LC-MS method 1: *m/z* 472.5 (MH⁺); RT (min) 4.24. LC-MS method 2: *m/z* 472.3 (MH⁺); RT (min) 2.85.

6-(4-Chlorophenyl)-3-[(1-isopropylpiperidin-3-yl)methyl]-2-(2-methylphenyl)quinazolin-4(3H)-one (9). To a mixture of **7** (200.0 mg, 0.45 mmol) and K_2CO_3 (249 mg, 1.80 mmol) in CH_3CN (20 mL) was added 2-iodopropane (0.05 mL, 0.54 mmol), and the reaction mixture was stirred at 70 °C for 14 h. The mixture was cooled to rt and concentrated under reduced pressure. The crude product was diluted with water (20 mL) and extracted with EtOAc (2 × 20 mL). The solvent was removed under reduced pressure, and the crude product was purified by HPLC using a gradient of 10−80% CH_3CN in water (0.1% TFA) to give the product (77 mg, 35%) as a light yellow oil. ^{1}H NMR (400 MHz, methanol-d_4): δ ppm 8.49 (t, *J* = 1.85 Hz, 1 H), 8.12 (dd, *J* = 8.58, 2.14 Hz, 1 H), 7.75 (dd, *J* = 8.38, 2.53 Hz, 3 H), 7.47−7.53 (m, 4 H), 7.42 (d, *J* = 7.80 Hz, 2 H), 7.39 (s, 1 H), 4.17 (dd, *J* = 13.74, 5.55 Hz, 1 H), 3.55 (dd, *J* = 13.54, 6.72 Hz, 1 H), 2.70−2.80 (m, 1 H), 2.63−2.70 (m, 1 H), 2.55 (d, *J* = 9.55 Hz, 1 H), 2.27 (d, *J* = 2.34 Hz, 3 H), 1.99−2.09 (m, 1 H), 1.87−1.98 (m, 1 H), 1.55−1.66 (m, 1 H), 1.39−1.46 (m, 1 H), 1.31−1.37 (m, 1 H), 0.94−1.04 (m, 6 H), 0.90 (dd, *J* = 12.38, 4.00 Hz, 1 H), 0.85 (dd, *J* = 8.19, 3.70 Hz,

1 H). LC-MS method 1: *m/z* 486.6 (MH+); RT (min) 4.26. LC-MS method 2: *m/z* 486.3 (MH+); RT (min) 2.91.

6-(4-Chlorophenyl)-3-[(1-cyclobutylpiperidin-3-yl)methyl]-2-(2-methylphenyl)quinazolin-4(3H)-one (10). ^{1}H NMR (400 MHz, methanol-d_4): δ ppm 8.42 (d, *J* = 1.17 Hz, 1 H), 8.05 (dd, *J* = 8.48, 2.05 Hz, 1 H), 7.64−7.70 (m, 3 H), 7.40−7.47 (m, 4 H), 7.32−7.37 (m, 2 H), 5.43 (s, 1 H), 4.05−4.16 (m, 1 H), 3.44−3.56 (m, 1 H), 2.64−2.75 (m, 1 H), 2.18−2.23 (m, 4 H), 2.13−2.16 (m, 1 H), 2.10 (dd, *J* = 10.43, 6.92 Hz, 1 H), 1.80−1.91 (m, 2 H), 1.49−1.60 (m, 3 H), 1.40 (ddd, *J* = 12.18, 8.38, 3.80 Hz, 1 H), 1.34 (s, 1 H), 0.82−0.87 (m, 1 H), 0.76−0.81 (m, 1 H), 0.34−0.45 (m, 1 H), 0.01 (t, *J* = 4.09 Hz, 1 H). LC-MS method 1: *m/z* 498.5 (MH+); RT (min) 4.32. LC-MS method 2: *m/z* 498.3 (MH+); RT (min) 2.96.

6-(4-Chlorophenyl)-3-{[1-(2-methoxyethyl)piperidin-3-yl]-methyl}-2-(2-methylphenyl)quinazolin-4(3H)-one (11). ^{1}H NMR (400 MHz, methanol-d_4): δ ppm 8.48 (s, 1 H), 8.11 (dd, *J* = 8.48, 2.24 Hz, 1 H), 7.71−7.76 (m, 3 H), 7.47−7.53 (m, 4 H), 7.37−7.43 (m, 2 H), 4.11−4.20 (m, 1 H), 3.55 (td, *J* = 13.20, 7.11 Hz, 1 H), 3.38−3.45 (m, 2 H), 3.29−3.35 (m, 3 H), 2.72−2.84 (m, 2 H), 2.42−2.51 (m, 2 H), 2.27 (d, *J* = 2.53 Hz, 3 H), 1.88−1.99 (m, 2 H), 1.51−1.63 (m, 2 H), 1.43−1.49 (m, 1 H), 1.38−1.43 (m, 1 H), 0.87 (td, *J* = 12.03, 3.80 Hz, 1 H). LC-MS method 1: *m/z* 502.5 (MH+); RT (min) 4.28. LC-MS method 2: *m/z* 502.3 (MH+); RT (min) 2.87.

6-(4-Chlorophenyl)-3-{[1-(2-fluoroethyl)piperidin-3-yl]methyl}-2-(2-methylphenyl)quinazolin-4(3H)-one (12). ^{1}H NMR (400 MHz, methanol-d_4): δ ppm 8.52 (d, *J* = 1.56 Hz, 1 H), 8.17 (d, *J* = 8.57 Hz, 1 H), 7.76 (m, 3 H), 7.52 (m, 4 H), 7.40−7.48 (m, 2 H), 4.80−4.88 (m, 1 H), 4.72 (d, *J* = 3.90 Hz, 1 H), 4.34 (dd, *J* = 13.84, 7.60 Hz, 1 H), 4.20 (dd, *J* = 14.03, 5.46 Hz, 1 H), 3.73 (dd, *J* = 13.74, 7.50 Hz, 1 H), 3.47−3.59 (m, 3 H), 3.39−3.47 (m, 2 H), 2.90 (d, *J* = 12.28 Hz, 1 H), 2.65−2.75 (m, 1 H), 2.22−2.32 (m, 3 H), 1.89−1.99 (m, 1 H), 1.62−1.73 (m, 1 H), 1.13−1.24 (m, 1 H). LC-MS method 1: *m/z* 490.4 (MH+); RT (min) 4.28. LC-MS method 2: *m/z* 490.2 (MH+); RT (min) 2.89.

6-(4-Chlorophenyl)-2-(2-methylphenyl)-3-{[1-(2,2,2-trifluoroethyl)piperidin-3-yl]methyl}quinazolin-4(3H)-one (13). ^{1}H NMR (400 MHz, methanol-d_4): δ ppm 8.51 (d, *J* = 1.96 Hz, 1 H), 8.15 (dd, *J* = 8.51, 1.27 Hz, 1 H), 7.72−7.79 (m, 3 H), 7.52 (d, *J* = 8.41 Hz, 3 H), 7.49 (d, *J* = 2.74 Hz, 1 H), 7.39−7.49 (m, 2 H), 4.20 (dd, *J* = 13.79, 6.94 Hz, 1 H), 4.12 (d, *J* = 6.26 Hz, 1 H), 3.81−3.83 (m, 1 H), 3.75−3.79 (m, 1 H), 3.64−3.73 (m, 2 H), 3.18−3.22 (m, 1 H), 3.12 (q, *J* = 9.72 Hz, 1 H), 3.00 (s, 1 H), 2.87−2.96 (m, 1 H), 2.35−2.47 (m, 1 H), 2.26−2.32 (m, 3 H), 2.10−2.14 (m, 1 H), 1.98−2.09 (m, 1 H), 1.95 (s, 1 H), 1.58−1.68 (m, 1 H), 1.43−1.54 (m, 1 H), 1.36 (d, *J* = 12.72 Hz, 1 H), 0.91−1.01 (m, 1 H). LC-MS method 1: *m/z* 526.3 (MH+); RT (min) 5.70. LC-MS method 2: *m/z* 526.2 (MH+); RT (min) 3.93.

6-(4-Chlorophenyl)-2-(2-methylphenyl)-3-{[1-(3,3,3-trifluoropropyl)piperidin-3-yl]methyl}quinazolin-4(3H)-one (14). ^{1}H NMR (400 MHz, methanol-d_4): δ ppm 8.53 (t, *J* = 2.25 Hz, 1 H), 8.14−8.21 (m, 1 H), 7.76 (d, *J* = 8.41 Hz, 3 H), 7.50−7.54 (m, 4 H), 7.40−7.47 (m, 2 H), 4.29−4.39 (m, 1 H), 4.16 (s, 1 H), 3.78 (s, 1 H), 3.58−3.65 (m, 2 H), 3.55 (d, *J* = 4.11 Hz, 1 H), 3.49 (dd, *J* = 3.42, 1.66 Hz, 1 H), 2.82−2.90 (m, 1 H), 2.75 (m, 2 H), 2.19−2.28 (m, 1 H), 1.90−2.00 (m, 1 H), 1.58−1.69 (m, 1 H), 1.36−1.46 (m, 1 H), 1.29−1.32 (m, 1 H), 1.12−1.23 (m, 1 H). LC-MS method 1: *m/z* (MH+) 540.5; RT (min) 4.39. LC-MS method 2: *m/z* 540.3 (MH+); RT (min) 3.04.

6-(4-Chlorophenyl)-3-[2-(1-ethylpiperidin-3-yl)ethyl]-2-(2-methoxyphenyl)quinazolin-4(3H)-one trifluoroacetate (15). ^{1}H NMR (300 MHz, methanol-d_4): δ ppm 8.50 (d, *J* = 1.47 Hz, 1 H), 8.14 (dd, *J* = 8.59, 2.28 Hz, 1 H), 7.72−7.79 (m, 3 H), 7.60−7.66 (m, 1 H), 7.49−7.55 (m, 3 H), 7.26 (d, *J* = 8.37 Hz, 1 H), 7.20 (td, *J* = 7.49, 0.88 Hz, 1 H), 4.20−4.35 (m, 1 H), 3.89 (s, 3 H), 3.80 (s, 1 H), 3.76 (ddd, *J* = 13.62, 3.08, 2.97 Hz, 1 H), 3.35−3.50 (m, 2 H), 3.05−3.14 (m, 2 H), 2.69−2.81 (m, 1 H), 2.45 (d, *J* = 11.45 Hz, 1 H), 1.89 (d, *J* = 14.53 Hz, 1 H), 1.71 (s, 1 H), 1.63 (d, *J* = 14.68 Hz, 4 H), 1.30 (td, *J* = 7.34, 0.88 Hz, 3 H).

LC-MS method 1: *m/z* 502.4 (MH+); RT (min) 4.27. LC-MS method 2: *m/z* 502.3 (MH+); RT (min) 2.88.

3-{[6-(4-Chlorophenyl)-2-(2-methylphenyl)-4-oxoquinazolin-3(4H)-yl]methyl}-1-ethylpyridinium iodide (17). To a solution of 6-bromo-2-(2-methylphenyl)-3-(pyridin-3-ylmethyl)quinazolin-4(3H)-one (16) (400 mg, 0.91 mmol) in acetone (20 mL) was added iodoethane (3.66 mL, 45.67 mmol), and the solution was stirred under nitrogen for 36 h at 50 °C in a sealed reaction tube. The mixture was cooled to rt and concentrated under reduced pressure, and the solid was washed with ether and dried in a high vacuum oven for 12 h. The obtained product (370 mg, 68%) was used in the next step without further purification. LC-MS method 2: *m/z* 438.3 (MH+); RT (min) 3.15.

6-(4-Chlorophenyl)-3-[(1-ethyl-1,2,5,6-tetrahydropyridin-3-yl)-methyl]-2-(2-methylphenyl)quinazolin-4(3H)-one (18). Compound 17 (370 mg, 0.62 mmol) was dissolved in a mixture of MeOH/CH$_2$Cl$_2$ (1:1). The solution was cooled to 0 °C, and NaBH$_4$ (189 mg, 4.98 mmol) was added. The reaction mixture was stirred at 0−5 °C for 3 h. Ice water was added, and the crude mixture was extracted with CH$_2$Cl$_2$ (2 × 50 mL). The combined organic layers were washed with brine, dried over Na$_2$SO$_4$, and filtered. The solvent was removed under reduced pressure and purified by HPLC with 10−80% CH$_3$CN in water (0.1% TFA) to give the product (56 mg, 17%) as a yellow oil. ^{1}H NMR (400 MHz, methanol-d_4): δ ppm 8.47−8.55 (m, 1 H), 8.13 (dd, *J* = 8.51, 2.25 Hz, 1 H), 7.73−7.80 (m, 3 H), 7.45−7.52 (m, 3 H), 7.39 (m, 3 H), 5.04 (s, 1 H), 4.73 (d, *J* = 15.65 Hz, 1 H), 4.26 (d, *J* = 15.65 Hz, 1 H), 2.71−2.80 (m, 1 H), 2.59−2.68 (m, 1 H), 2.40−2.51 (m, 4 H), 2.24−2.31 (m, 3 H), 2.09 (d, *J* = 1.37 Hz, 2 H), 1.06 (t, *J* = 7.14 Hz, 3 H). LC-MS method 1: *m/z* 470.3 (MH+); RT (min) 4.25. LC-MS method 2: *m/z* 470.2 (MH+); RT (min) 2.85.

3-[(4-Benzylmorpholin-2-yl)methyl]-6-bromo-2-(2-methylphenyl)quinazolin-4(3H)-one (20). 1-(4-Benzylmorpholin-2-yl)methanamine (2.00 g, 9.70 mmol) in toluene (15 mL) was added to compound 3 (2.55 g, 8.08 mmol), and the solution was stirred at reflux for 16 h under a nitrogen atmosphere. The mixture was concentrated under reduced pressure and passed through a silica gel plug (100% EtOAc). The resulting intermediate (yellow oil) (2.50 g, 4.79 mmol) was added to a dry round-bottom flask followed by ethylene glycol (20 mL) and LiOH (0.40 g, 9.57 mmol). The resulting mixture was stirred at 135 °C for 16 h. This mixture was cooled to rt, diluted with CH$_2$Cl$_2$ and water, and extracted with CH$_2$Cl$_2$ (2 × 50 mL). The combined organic fractions were concentrated under reduced pressure. The residue was purified by silica gel flash chromatography using a gradient of 10−50% ethyl acetate in hexanes to afford 1.62 g (67%) of the product. ^{1}H NMR (400 MHz, methanol-d_4): δ ppm 8.49 (d, *J* = 1.56 Hz, 1 H), 8.10−8.15 (m, 1 H), 7.71−7.77 (m, 3 H), 7.44−7.52 (m, 4 H), 7.33−7.41 (m, 2 H), 4.26 (dd, *J* = 13.45, 3.51 Hz, 1 H), 3.99−4.11 (m, 1 H), 3.81−3.88 (m, 1 H), 3.70−3.79 (m, 2 H), 3.42 (tt, *J* = 11.42, 2.41 Hz, 1 H), 2.71−2.80 (m, 1 H), 2.57 (dt, *J* = 13.11, 6.60 Hz, 1 H), 2.30−2.37 (m, 1 H), 2.12−2.23 (m, 3 H), 1.76−1.83 (m, 1 H), 1.03 (dd, *J* = 6.43, 1.95 Hz, 6 H). LC-MS method 2: *m/z* 504.3 (MH+); RT (min) 2.83.

3-[(4-Benzylmorpholin-2-yl)methyl]-6-(4-chlorophenyl)-2-(2-methylphenyl)quinazolin-4(3H)-one (21). To a dry 100 mL round-bottom flask was 20 (2.44 g, 4.84 mmol) followed by anhydrous toluene (20.0 mL), dioxane (5.00 mL), and water (2.5 mL). The mixture was stirred under a nitrogen atmosphere, and 4-chlorophenyl boronic acid (756 mg, 4.84 mmol), K$_2$CO$_3$ (4.01 g, 29.0 mmol), and PdCl$_2$(dppf) (395 mg, 0.48 mmol) were added. The reaction mixture was heated to 90 °C for 12 h and then filtered through a silica gel plug with EtOAc as the eluent (60 mL). Removal of the solvent under reduced pressure and purification of the residue by silica gel flash chromatography (80% hexanes:20% EtOAc) gave the product as a light yellow solid (1.99 g, 76%). ^{1}H NMR (400 MHz, methanol-d_4): δ ppm 8.46−8.48 (m, 1 H), 8.10−8.12 (dd, 1 H), 7.72−7.75 (m, 3 H), 7.49−7.51 (d, 3 H), 7.35−7.36 (m, 3 H), 7.25−7.28 (m, 5 H), 4.18−4.22 (m, 1 H), 3.65−4.08 (m, 3 H), 3.30−3.48 (m, 3 H), 2.55−2.71 (m, 2 H), 2.20−2.31 (d, 3 H),

2.00–2.08 (m, 1 H), 1.63–1.69 (m, 1 H). LC-MS method 2: m/z 536.2 (MH$^+$); RT (min) 2.89.

6-(4-Chlorophenyl)-2-(2-methylphenyl)-3-(morpholin-2-yl-methyl)quinazolin-4(3H)-one (22). A solution of **21** (2.59 g, 4.84 mmol) in 1,2-dichloroethane (25 mL) was treated with 1-chlorom-ethyl chloroformate (1.32 mL, 12.1 mmol) at rt for 30 min. The reaction mixture was then heated under reflux for 2 h. The solvent was evaporated under reduced pressure, and the residue was heated in MeOH (20 mL) under reflux for another 2 h. The solvent was removed under reduced pressure, and the residue was triturated with hexane. The residue was washed with diethylether to provide the product (1.96 g, 91%) as a white solid. LC-MS method 2: m/z 446.1 (MH$^+$); RT (min) 2.63.

6-(4-Chlorophenyl)-3-[(4-isopropylmorpholin-2-yl)methyl]-2-(2-methylphenyl)quinazolin-4(3H)-one (23). Starting from com-pound **21**, the title compound was prepared using the same procedure as used for the preparation of compound **9**. ^{1}H NMR (400 MHz, methanol-d_4): δ ppm 8.49 (d, J = 1.56 Hz, 1 H), 8.10–8.15 (m, 1 H), 7.71–7.77 (m, 3 H), 7.44–7.52 (m, 4 H), 7.33–7.41 (m, 2 H), 4.26 (dd, J = 13.45, 3.51 Hz, 1 H), 3.99–4.11 (m, 1 H), 3.81–3.88 (m, 1 H), 3.70–3.79 (m, 2 H), 3.42 (tt, J = 11.42, 2.41 Hz, 1 H), 2.71–2.80 (m, 1 H), 2.57 (dt, J = 13.11, 6.60 Hz, 1 H), 2.30–2.37 (m, 1 H), 2.12–2.23 (m, 3 H), 1.76–1.83 (m, 1 H), 1.03 (dd, J = 6.43, 1.95 Hz, 6 H). LC-MS method 1: m/z 488.5 (MH$^+$); RT (min) 4.26. LC-MS method 2: m/z 488.3 (MH$^+$); RT (min) 2.85.

6-(4-Chlorophenyl)-3-{[(3S)-1-ethylpiperidin-3-yl]methyl}-2-(2-methylphenyl)quinazolin-4(3H)-one (24). ^{1}H NMR (400 MHz, methanol-d_4): δ ppm 8.49 (d, J = 1.57 Hz, 1 H), 8.13 (dd, J = 8.41, 2.15 Hz, 1 H), 7.75 (dd, J = 8.31, 2.05 Hz, 3 H), 7.47–7.53 (m, 4 H), 7.38–7.44 (m, 2 H), 4.15–4.21 (m, 1 H), 3.52–3.62 (m, 1 H), 2.84 (t, J = 9.49 Hz, 1 H), 2.76 (d, J = 10.96 Hz, 1 H), 2.32–2.41 (m, 2 H), 2.28 (d, J = 4.89 Hz, 3 H), 1.89–1.99 (m, 1 H), 1.80–1.89 (m, 1 H), 1.53–1.64 (m, 2 H), 1.41–1.47 (m, 1 H), 1.32–1.39 (m, 1 H), 1.02 (dt, J = 9.78, 7.24 Hz, 3 H), 0.89–0.96 (m, 1 H). LC-MS method 1: m/z 472.5 (MH$^+$); RT (min) 4.24. LC-MS method 2: m/z 472.3 (MH$^+$); RT (min) 2.86.

6-(4-Chlorophenyl)-3-{[(3R)-1-ethylpiperidin-3-yl]methyl}-2-(2-methylphenyl)quinazolin-4(3H)-one (25). ^{1}H NMR (400 MHz, methanol-d_4): δ ppm 8.50 (d, J = 1.56 Hz, 1 H), 8.13 (dd, J = 8.61, 2.15 Hz, 1 H), 7.75 (dd, J = 8.51, 2.45 Hz, 3 H), 7.51 (ddd, J = 11.30, 4.65, 2.25 Hz, 4 H), 7.38–7.44 (m, 2 H), 4.13–4.23 (m, 1 H), 3.52–3.62 (m, 1 H), 2.84–2.91 (m, 2 H), 2.41 (dq, J = 13.60, 6.81 Hz, 2 H), 2.28 (d, J = 5.48 Hz, 3 H), 1.90–2.00 (m, J = 10.83, 7.15, 7.15, 3.42 Hz, 2 H), 1.57–1.68 (m, 2 H), 1.40–1.48 (m, 1 H), 1.33–1.38 (m, 1 H), 1.04 (dt, J = 11.35, 7.24 Hz, 3 H), 0.88–0.97 (m, 1 H). LC-MS method 1: m/z 472.5 (MH$^+$); RT (min) 4.26. LC-MS method 2: m/z 472.3 (MH$^+$); RT (min) 2.86.

6-(4-Fluorophenyl)-2-isopropyl-3-[(1-isopropylpiperidin-3-yl)-methyl]quinazolin-4(3H)-one (26). ^{1}H NMR (400 MHz, dichloro-methane-d_2): δ ppm 8.40 (d, J = 2.15 Hz, 1 H), 7.93 (dd, J = 8.51, 2.25 Hz, 1 H), 7.65–7.72 (m, 3 H), 7.15–7.22 (m, 2 H), 4.07–4.18 (m, 2 H), 3.31 (dt, J = 13.06, 6.48 Hz, 1 H), 2.72 (m, 3 H), 2.29 (m, 1 H), 2.18 (m, 1 H), 2.03 (m, 1 H), 1.66–1.77 (m, 2 H), 1.49–1.61 (m, 1 H), 1.39 (t, J = 6.46 Hz, 6 H), 1.21–1.32 (m, 1 H), 0.97–1.07 (m, 6 H). LC-MS method 1: m/z 422.4 (MH$^+$); RT (min) 4.20. LC-MS method 2: m/z 422.3 (MH$^+$); RT (min) 2.57.

6-(4-Chlorophenyl)-2-isopropyl-3-{[(3S)-1-isopropylpiperidin-3-yl]methyl}quinazolin-4(3H)-one (27). ^{1}H NMR (400 MHz, dichloromethane-d_2): δ ppm 8.42 (d, J = 2.14 Hz, 1 H), 7.94 (dd, J = 8.48, 2.24 Hz, 1 H), 7.65–7.73 (m, 3 H), 7.46 (ddd, J = 8.92, 2.63, 2.29 Hz, 2 H), 4.12 (m, 2 H), 3.43 (d, J = 4.09 Hz, 1 H), 2.68 (m, 2 H), 2.32 (m, 1 H), 2.20–2.30 (m, 1 H), 2.13 (m, 1 H), 1.90–1.98 (m, 1 H), 1.70 (m, 2 H), 1.39 (t, J = 6.43 Hz, 6 H), 1.24–1.32 (m, 1 H), 1.22 (dd, J = 8.96, 4.48 Hz, 1 H), 1.00 (m, 6 H). LC-MS method 1: m/z 438.5 (MH$^+$); RT (min) 4.27. LC-MS method 2: m/z 438.3 (MH$^+$); RT (min) 2.90.

7-(4-Chlorophenyl)-3-[(1-ethylpiperidin-3-yl)methyl]-2-(2-methoxyphenyl)quinazolin-4(3H)-one trifluoroacetate (28). ^{1}H

NMR (300 MHz, methanol-d_4): δ ppm 8.31–8.39 (m, 1 H), 7.82–7.91 (m, 2 H), 7.74 (d, J = 8.51 Hz, 2 H), 7.63 (td, J = 6.46, 1.76 Hz, 1 H), 7.48–7.60 (m, 3 H), 7.16–7.28 (m, 2 H), 4.20–4.40 (m, 1 H), 3.90 (s, 3 H), 3.00–3.80 (m, 5 H), 2.40–2.80 (m, 3 H), 1.00–2.00 (m, 7 H). LC-MS method 1: m/z 488.4 (MH$^+$); RT (min) 4.24. LC-MS method 2: m/z 488.3 (MH$^+$); RT (min) 2.88.

3-[(1-Isopropylpiperidin-3-yl)methyl]-2-(2-methylphenyl)-quinazolin-4(3H)-one (29). ^{1}H NMR (400 MHz, methanol-d_4): δ ppm 8.28 (d, J = 7.99 Hz, 1 H), 7.82–7.87 (m, 1 H), 7.67 (d, J = 8.19 Hz, 1 H), 7.59 (t, J = 7.50 Hz, 1 H), 7.46–7.52 (m, 2 H), 7.37–7.43 (m, 2 H), 4.16 (dd, J = 7.70, 5.94 Hz, 1 H), 4.13 (d, J = 1.75 Hz, 1 H), 3.52 (dd, J = 13.54, 6.92 Hz, 1 H), 2.75 (t, J = 10.33 Hz, 1 H), 2.60–2.69 (m, 2 H), 2.26 (d, J = 1.95 Hz, 3 H), 2.02 (t, J = 11.50 Hz, 1 H), 1.87–1.92 (ddd, J = 10.52, 7.21, 3.70 Hz, 1 H), 1.62 (tt, J = 10.52, 3.80 Hz, 1 H), 1.38–1.46 (m, 1 H), 1.31–1.36 (m, 1 H), 0.95–1.02 (m, 6 H), 0.82–0.90 (m, J = 12.11, 12.11, 4.04, 3.90 Hz, 1 H). LC-MS method 1: m/z 376.4 (MH$^+$); RT (min) 3.81. LC-MS method 2: m/z 376.3 (MH$^+$); RT (min) 2.22.

3-[(1-Ethylpiperidin-3-yl)methyl]-6-methoxy-2-(2-methoxy-phenyl)quinazolin-4(3H)-one trifluoroacetate (30). ^{1}H NMR (300 MHz, methanol-d_4): δ ppm 7.59–7.72 (m, 3 H), 7.46–7.56 (m, 2 H), 7.21–7.28 (m, 1 H), 7.15–7.21 (m, 1 H), 4.20–4.50 (m, 1 H), 3.95 (s, 3 H), 3.90 (s, 3 H), 3.40–3.89 (m, 3 H), 3.10 (m, 2 H), 2.40–2.80 (m, 2 H), 2.00–2.25 (brs, 1 H), 1.00–2.00 (m, 7 H). LC-MS method 1: m/z 408.3 (MH$^+$); RT (min) 3.82. LC-MS method 2: m/z 408.3 (MH$^+$); RT (min) 2.23.

3-[(1-Ethylpiperidin-3-yl)methyl]-2-(2-methylphenyl)-6-(tri-fluoromethoxy)quinazolin-4(3H)-one (31). ^{1}H NMR (400 MHz, methanol-d_4): δ ppm 8.11 (s, 1 H), 7.74–7.79 (m, 2 H), 7.49 (t, J = 7.21 Hz, 2 H), 7.37–7.43 (m, 2 H), 4.14 (dd, J = 13.64, 6.82 Hz, 1 H), 3.52–3.61 (m, 1 H), 2.79–2.87 (m, 1 H), 2.58 (m, 1 H), 2.32–2.41 (m, 2 H), 2.26 (d, J = 4.48 Hz, 3 H), 1.85–1.96 (m, J = 18.22, 11.01, 3.90, 3.70 Hz, 1 H), 1.84 (s, 1 H), 1.51–1.60 (m, 1 H), 1.31–1.38 (m, 1 H), 1.02 (dt, J = 10.13, 7.21 Hz, 3 H), 0.89 (ddd, J = 18.32, 12.08, 4.09 Hz, 1 H). LC-MS method 1: m/z 446.5 (MH$^+$); RT (min) 4.05. LC-MS method 2: m/z 446.3 (MH$^+$); RT (min) 2.57.

***tert*-Butyl 3-{[6-bromo-2-(2-methylphenyl)-4-oxoquinazolin-3(4H)-yl]methyl}piperidine-1-carboxylate (32).** *tert*-Butyl 3-(ami-nomethyl)piperidine-1-carboxylate (3.00 g, 14.0 mmol) in toluene (20 mL) was added to 6-bromo-2-(2-methylphenyl)-4H-3,1-ben-zoxazin-4-one (3.69 g, 11.7 mmol) (**3**), and the solution was stirred at reflux for 16 h under a nitrogen atmosphere. The mixture was concentrated under reduced pressure and passed through a silica gel plug using EtOAc as the eluent. Removal of the solvent under reduced pressure gave the intermediate as a yellow oil, which was used in the next step without further purification.

The intermediate described above (3.00 g, 5.66 mmol) was added to a dry round-bottom flask followed by ethylene glycol (20 mL) and LiOH (0.48 g, 11.3 mmol). The resulting mixture was stirred at 135 °C for 16 h, cooled to rt, and diluted with CH$_2$Cl$_2$ and water. The mixture was extracted with CH$_2$Cl$_2$ (50 mL × 2), and the combined organic layers were concentrated under reduced pressure. Purification via silica gel column chromatography using a gradient elution from 10 to 50% ethyl acetate in hexanes yielded the product (1.4 g, 48%). LC-MS method 2: m/z 512.5 (MH$^+$); RT (min) 4.01

***tert*-Butyl 3-{[6-(4-fluorophenoxy)-2-(2-methylphenyl)-4-oxo-quinazolin-3(4H)-yl]methyl}piperidine-1-carboxylate (33).** Under a nitrogen atmosphere, 4-fluorophenol (210 mg, 1.87 mmol), **32** (800 mg, 1.56 mmol), copper(I) chloride (77.3 mg, 0.78 mmol), 2,2,6,6-tetramethylheptane-3,5-dione (TMHD) (116 mg, 0.39 mmol), and Cs$_2$CO$_3$ (1.02 g, 3.12 mmol) were combined in a flask, and 1-methyl-2-pyrrolidone (2 mL) was added. The reaction mixture was stirred for 12 h at 120 °C, cooled, and concentrated under reduced pressure. The crude product was purified by HPLC to give the product (392 mg, 46%).

6-(4-Fluorophenoxy)-2-(2-methylphenyl)-3-(piperidin-3-yl-methyl)quinazolin-4(3H)-one (34). Compound **33** (573.6 mg, 1.06 mmol) was dissolved in CH$_2$Cl$_2$ (5 mL), and TFA (5 mL) was added. After it was stirred for 3 h at rt, the solvent was removed.

Saturated aqueous NaHCO$_3$ solution was added, and the product was extracted with EtOAc (2×). The combined organic layers were dried with Na$_2$SO$_4$ and filtered, and the solvent was removed under reduced pressure to give the product as an oil (371 mg, 79%). ^{1}H NMR (400 MHz, methanol-d_4): δ ppm 7.68 (d, J = 9.00 Hz, 1 H), 7.60 (d, J = 2.74 Hz, 1 H), 7.53 (dd, J = 8.80, 2.74 Hz, 1 H), 7.45−7.50 (m, 2 H), 7.35−7.43 (m, 2 H), 7.11−7.20 (m, 4 H), 4.02−4.15 (dd, J = 13.60, 7.73 Hz, 1 H), 3.42−3.60 (dd, J = 13.50, 8.02 Hz, 1 H), 2.85 (d, J = 12.32 Hz, 1 H), 2.79 (dd, J = 12.32, 2.74 Hz, 1 H), 2.42 (qd, J = 11.80, 2.74 Hz, 1 H), 2.20−2.26 (m, 3 H), 2.11 (dd, J = 12.03, 10.66 Hz, 1 H), 1.78 (ddd, J = 10.32, 6.80, 3.23 Hz, 1 H), 1.51−1.61 (m, 2 H), 1.28−1.39 (m, 2 H), 0.93−1.04 (m, 1 H). LC-MS method 1: m/z 444.4 (MH$^+$); RT (min) 4.16. LC-MS method 2: m/z 444.2 (MH$^+$); RT (min) 2.74.

6-(4-Fluorophenoxy)-3-[(1-isopropylpiperidin-3-yl)methyl]-2-(2-methylphenyl)quinazolin-4(3H)-one (35). Compound **34** (200 mg, 0.45 mmol), 2-iodopropane (91.9 mg, 0.54 mmol), and K$_2$CO$_3$ (249 mg, 1.8 mmol) were combined in acetonitrile and heated to 70 °C for 16 h. The solid was filtered off, and the filtrate was concentrated under reduced pressure. Saturated aqueous NaHCO$_3$ solution was added, and the product was extracted with EtOAc (2×). The combined organic layers were dried with Na$_2$SO$_4$ and filtered, and the solvent was removed under reduced pressure to give the product (188 mg, 86%). ^{1}H NMR (400 MHz, methanol-d_4): δ ppm 7.68 (d, J = 8.80 Hz, 1 H), 7.60 (d, J = 2.74 Hz, 1 H), 7.45−7.54 (m, 3 H), 7.36−7.41 (m, 2 H), 7.10−7.19 (m, 4 H), 4.06−4.15 (m, 1 H), 3.45−3.55 (m, 1 H), 2.72 (t, J = 9.68 Hz, 1 H), 2.59−2.67 (m, 2 H), 2.19−2.29 (m, 3 H), 1.96−2.03 (m, 1 H), 1.82−1.93 (m, 2 H), 1.58−1.63 (m, 1 H), 1.55 (dd, J = 7.04, 4.11 Hz, 1 H), 1.27−1.34 (m, 1 H), 0.92−1.02 (m, 6 H), 0.78−0.84 (m, 1 H). LC-MS method 1: m/z 486.4 (MH$^+$); RT (min) 4.28. LC-MS method 2: m/z 486.4 (MH$^+$); RT (min) 2.92.

6-(4-Fluorophenoxy)-3-{[(3S)-1-isopropylpiperidin-3-yl]methyl}-2-(2-methylphenyl)quinazolin-4(3H)-one (36). ^{1}H NMR (400 MHz, methanol-d_4): δ ppm 7.69 (d, J = 8.77 Hz, 1 H), 7.62 (d, J = 2.73 Hz, 1 H), 7.53−7.57 (m, 1 H), 7.45−7.50 (m, 2 H), 7.37−7.42 (m, 2 H), 7.13−7.22 (m, 4 H), 4.12 (dt, J = 13.30, 5.63 Hz, 1 H), 3.50 (dd, J = 13.54, 7.11 Hz, 1 H), 2.75 (t, J = 10.62 Hz, 1 H), 2.65 (td, J = 12.28, 6.63 Hz, 2 H), 2.24 (d, J = 1.75 Hz, 3 H), 1.99−2.06 (m, 1 H), 1.83−1.94 (m, 2 H), 1.57−1.65 (m, 1 H), 1.36−1.45 (m, J = 16.83, 8.40, 4.04, 4.04 Hz, 1 H), 1.34−1.36 (m, 1 H), 0.95−1.02 (m, 6 H), 0.80−0.91 (m, 1 H). LC-MS method 1: m/z 486.6 (MH$^+$); RT (min) 4.2. LC-MS method 2: m/z 486.3 (MH$^+$); RT 2.78 (min).

6-(4-Fluorophenoxy)-2-isopropyl-3-[(1-isopropylpiperidin-3-yl)methyl]quinazolin-4(3H)-one (37). ^{1}H NMR (400 MHz, dichloromethane-d_2): δ ppm 7.76−7.85 (m, 1 H), 7.57−7.65 (m, 1 H), 7.48−7.56 (m, J = 5.87, 2.98, 2.98, 2.98, 2.98 Hz, 1 H), 7.04−7.16 (m, 4 H), 4.26 (d, J = 7.63 Hz, 1 H), 4.10 (dd, J = 14.28, 5.87 Hz, 1 H), 3.41−3.51 (m, 3 H), 3.17−3.27 (m, J = 6.75, 6.75, 6.75, 6.75, 6.75, 6.75 Hz, 1 H), 2.69−2.80 (m, 2 H), 2.50−2.61 (m, 1 H), 1.97−2.07 (m, 2 H), 1.87−1.95 (m, 1 H), 1.44−1.50 (m, 5 H), 1.38−1.42 (m, 1 H), 1.33 (dd, J = 12.23, 6.75 Hz, 5 H). LC-MS method 1: m/z 438.6 (MH$^+$); RT (min) 4.18. LC-MS method 2: m/z 438.3 (MH$^+$); RT (min) 2.76.

***tert*-Butyl (3R)-3-{[(2-amino-5-bromobenzoyl)amino]methyl}-piperidine-1-carboxylate (38).** A mixture of 5-bromoisatoic anhydride (20.3 g, 84 mmol), *tert*-butyl (3*R*)-3-(aminomethyl)-piperidine-1-carboxylate **5a** (15.0 g, 70.0 mmol), potassium carbonate (19.3 g, 140 mmol), and THF (100 mL) was heated to 70 °C for 20 h, followed by cooling to room temperature and the addition of water to give a clear biphasic solution. Stirring was continued for 4 h, and most of the organic solvent was removed under reduced pressure. The solid was collected by filtration, washed with a copious amount of water, and air-dried to give 24.9 g (86%) of product. LC-MS method 2: m/z 312.3 ([MH$_2$− BOC]$^+$); RT (min) 3.26.

***tert*-Butyl (3R)-3-[(6-bromo-2-methyl-4-oxoquinazolin-3(4H)-yl)methyl]piperidine-1-carboxylate (39).** A mixture of compound **38** (10 g, 24.3 mmol) and triethyl orthoacetate (30 mL) was heated to 140 °C for 10 h while stirring. The excess triethyl orthoacetate

was then removed under reduced pressure to give the product, which was used in the next step without further purification. LC-MS method 2: m/z 338.4 ([MH$_2$ − BOC]$^+$); RT (min) 3.47.

6-Bromo-2-methyl-3-[(3S)-piperidin-3-ylmethyl]quinazolin-4(3H)-one (40). Compound **39** was treated with 20% TFA in CH$_2$Cl$_2$ (30 mL) at rt for 15 h. The solvent and excess TFA were removed under reduced pressure.

6-Bromo-3-{[(3S)-1-isopropylpiperidin-3-yl]methyl}-2-methylquinazolin-4(3H)-one (41). Intermediate **40** was treated with K$_2$CO$_3$ (16.8 g, 121 mmol) and 2-iodopropane (6.2 g, 36 mmol) in acetonitrile (50 mL) at 70 °C for 15 h. The mixture was then cooled to room temperature and diluted with water (200 mL) and EtOAc (400 mL) to give a clear biphasic solution. The organic layer was separated and washed with water and brine, dried over magnesium sulfate, filtered, and evaporated to give 7.36 g of product (80% from three steps). LC-MS method 2: m/z 378.3 (MH$^+$); RT (min) 1.95.

6-(4-Chlorophenyl)-3-{[(3S)-1-isopropylpiperidin-3-yl]methyl}-2-methylquinazolin-4(3H)-one (42). A mixture of compound **41** (6.2 mmol, 2.34 g), 4-chlorophenyl boronic acid (9.3 mmol, 1.45 g), cesium carbonate (12.4 mmol, 4.03 g), and 1,1′-bis(diphenylphosphino)ferrocenepalladium(II) chloride dichloromethane adduct (0.37 mmol, 0.3 g) in 1,2-dimethoxyethane (15 mL) and water (5 mL) was degassed, flashed with nitrogen, and heated to 60 °C for 12 h. The mixture was filtered, and the filtrate was separated by preparative HPLC using 0.1% NH$_3$ in water and 0.1% NH$_3$ in acetonitrile as the eluent (gradient from 25 to 80%) to afford pure product (1.6 g, 63%). ^{1}H NMR (400 MHz, chloroform-d): δ ppm 8.41 (d, J = 1.96 Hz, 1 H), 7.92 (dd, J = 8.51, 2.25 Hz, 1 H), 7.67 (d, J = 8.41 Hz, 1 H), 7.61 (ddd, J = 8.90, 2.54, 2.25 Hz, 2 H), 7.43 (ddd, J = 8.85, 2.45, 2.20 Hz, 2 H), 4.03−4.14 (m, 2 H), 2.86 (d, J = 8.41 Hz, 1 H), 2.67−2.79 (m, 5 H), 2.23 (d, J = 4.89 Hz, 1 H), 2.17 (m, 1 H), 1.75 (m, 2 H), 1.54 (d, J = 6.46 Hz, 1 H), 1.21−1.32 (m, 1 H), 1.15 (d, J = 6.85 Hz, 1 H), 1.05 (s, 6 H). LC-MS method 1: m/z 410.3 (MH$^+$); RT (min) 4.10. LC-MS method 2: m/z 410.2 (MH$^+$); RT (min) 2.60.

6-(4-Fluorophenoxy)-3-{[(3S)-1-isopropylpiperidin-3-yl]methyl}-2-methylquinazolin-4(3H)-one (43). To a microwave reactor tube was added compound **41** (620 mg, 1.64 mmol), 4-fluorophenol (220 mg, 1.97 mmol), cesium carbonate (1.6 g, 4.92 mmol), copper(I) chloride (64.9 mg, 0.66 mmol), TMHD (97.7 mg, 0.33 mmol), and NMP (8 mL). The tube was then sealed, degassed, flashed with nitrogen, and heated to 205 °C in a microwave reactor ["Emrys Optimizer" from Personal Chemistry (now Biotage)] for 20 min. The reaction mixture was filtered, and the filtrate was purified using a Gilson reversed-phase HPLC system with a gradient elution from 5 to 60% acetonitrile in water containing 1% TFA. The product fractions were combined, treated with 10% Na$_2$CO$_3$, and extracted with EtOAc (3×). The extract was then washed with water and brine, dried over MgSO$_4$, and evaporated to afford 255 mg (38%) of the title product. ^{1}H NMR (400 MHz, CD$_2$Cl$_2$): δ ppm 7.55−7.60 (m, 2H), 7.39 (dd, 1H), 7.15−7.00 (m, 4H), 3.96 (d, 2H), 2.75−2.61 (m, 3H), 2.60 (s, 3H), 2.22 (t, 1H), 2.11−2.02 (m, 2 H), 1.78−1.54 (m, 2H), 1.49−1.40 (m, 1H), 1.21−1.09 (m, 1H), 0.95 (d, 6H). LC-MS method 1: m/z 410.5 (MH$^+$); RT (min) 3.99. LC-MS method 2: m/z 410.2 (MH$^+$); RT (min) 2.44.

6-(4-Chlorophenyl)-3-[(1-isopropylpiperidin-3-yl)methyl]quinazolin-4(3H)-one (44). ^{1}H NMR (400 MHz, methanol-d_4): δ ppm 8.47 (d, J = 2.14 Hz, 1 H), 8.33 (s, 1 H), 8.13 (dd, J = 8.57, 2.14 Hz, 1 H), 7.80 (d, J = 8.38 Hz, 1 H), 7.69−7.75 (m, 2 H), 7.50 (d, J = 8.38 Hz, 2 H), 4.11−4.18 (m, 1 H), 3.98−4.05 (m, 1 H), 3.49−3.58 (m, 1 H), 3.44 (d, J = 11.89 Hz, 2 H), 2.93−3.01 (m, 2 H), 2.47 (m, 1 H), 2.08 (d, J = 14.42 Hz, 1 H), 1.95 (m, 1 H), 1.79 (d, J = 14.23 Hz, 1 H), 1.35−1.45 (m, 7 H). LC-MS method 1: m/z 396.4 (MH$^+$); RT (min) 4.07. LC-MS method 2: m/z 396.3 (MH$^+$); RT (min) 2.56.

6-(4-Fluorophenoxy)-3-{[(3S)-1-isopropylpiperidin-3-yl]methyl}quinazolin-4(3H)-one (45). ^{1}H NMR (400 MHz, methanol-d_4): δ ppm 8.19−8.23 (m, 1 H), 7.70 (d, J = 8.77 Hz, 1 H), 7.49−7.57 (m, 2 H), 7.09−7.19 (m, 4 H), 3.88−3.99 (m, 2 H), 2.75−2.84 (m, 2 H), 2.70−2.73 (m, 1 H), 2.20 (td, J = 11.55, 2.44 Hz,

1 H), 2.13 (td, $J = 6.97, 3.41$ Hz, 1 H), 2.06 (d, $J = 10.52$ Hz, 1 H), 1.68−1.79 (m, 2 H), 1.49−1.60 (m, 1 H), 1.11 (dd, $J = 11.60, 3.02$ Hz, 1 H), 1.05 (dd, $J = 6.43, 5.07$ Hz, 6 H). LC-MS method 1: m/z 396.5 (MH$^+$); RT (min) 3.96. LC-MS method 2: m/z 396.2 (MH$^+$); RT (min) 2.43.

2-[2-Fluoro-4-(2-hydroxyethoxy)phenyl]-6-(4-fluorophenoxy)-3-[(1-isopropylpiperidin-3-yl)methyl]quinazolin-4(3H)-one (46). The synthesis is described in the Supporting Information. ^{1}H NMR (300 MHz, methanol-d_4): δ ppm 7.69 (t, $J = 8.07$ Hz, 1 H), 7.49−7.61 (m, 3 H), 7.10−7.22 (m, 4 H), 6.90−7.04 (m, 2 H), 4.07−4.21 (m, 3 H), 3.86−3.97 (m, 2 H), 3.73 (m, 1 H), 2.64 (m, 3 H), 1.96−2.10 (m, 1 H), 1.91 (m, 2 H), 1.57 (m, 2 H), 1.39 (m, 2 H), 0.96 (m, 6 H). LC-MS method 1: m/z 550.3 (MH$^+$); RT (min) 4.16. LC-MS method 2: m/z 550.3 (MH$^+$); RT (min) 2.71.

Supporting Information Available: Synthetic procedures for the preparation of compounds **1**, **2**, and **46**. Comparison of the ghrelin binding affinities of multiple enantiomeric pair members. Analytical data and purity assessment of key compounds. This material is available free of charge via the Internet at http://pubs.acs.org.

References

(1) Gan, D. *Diabetes Atlas*, 2nd ed.; International Diabetes Federation: Brussels, 2003.

(2) Bailey, C. J. Drugs on the horizon for diabesity. *Curr. Diabetes Rep.* **2005**, *5*, 353−359.

(3) van der Lely, A. J.; Tschop, M.; Heiman, M. L.; Ghigo, E. Biological, physiological, pathophysiological, and pharmacological aspects of ghrelin. *Endocr. Rev.* **2004**, *25*, 426−457.

(4) Cummings, D. E.; Overduin, J.; Foster-Schubert, K. E. Roles for ghrelin in the regulation of appetite and body weight. *Curr. Opin. Endocrinol. Diabetes* **2005**, *12*, 72−79.

(5) Popovic, V. Ghrelin. *Curr. Opin. Endocrinol. Diabetes* **2006**, *13*, 70−75.

(6) Zhao, H.; Liu, G. Growth hormone secretagogue receptor antagonists as anti-obesity therapies? Still an open question. *Curr. Opin. Drug Discovery Dev.* **2006**, *9*, 509−515.

(7) Volante, M.; Allia, E.; Gugliotta, P.; Funaro, A.; Broglio, F.; et al. Expression of and of the GH secretagogue receptor by pancreatic islet cells and related endocrine tumors. *J. Clin. Endocrinol. Metab.* **2002**, *87*, 1300−1308.

(8) Adeghate, E.; Ponery, A. S. Ghrelin stimulates insulin secretion from the pancreas of normal and diabetic rats. *J. Neuroendocrinol.* **2002**, *14*, 555−560.

(9) Wierup, N.; Svensson, H.; Mulder, H.; Sundler, F. The ghrelin cell: A novel developmentally regulated islet cell in the human pancreas. *Regul. Pept.* **2002**, *107*, 63−69.

(10) Date, Y.; Nakazato, M.; Hashiguchi, S.; Dezaki, K.; Mondal, M. S.; et al. Ghrelin is present in pancreatic alpha-cells of humans and rats and stimulates insulin secretion. *Diabetes* **2002**, *51*, 124−129.

(11) Wierup, N.; Yang, S.; McEvilly, R. J.; Mulder, H.; Sundler, F. Ghrelin is expressed in a novel endocrine cell type in developing rat islets and inhibits insulin secretion from INS-1 (832/13) cells. *J. Histochem. Cytochem.* **2004**, *52*, 301−310.

(12) Dezaki, K.; Hosoda, H.; Kakei, M.; Hashiguchi, S.; Watanabe, M.; et al. Endogenous ghrelin in pancreatic islets restricts insulin release by attenuating Ca^{2+} signaling in beta-cells: Implication in the glycemic control in rodents. *Diabetes* **2004**, *53*, 3142−3151.

(13) Kageyama, H.; Funahashi, H.; Hirayama, M.; Takenoya, F.; Kita, T.; et al. Morphological analysis of ghrelin and its receptor distribution in the rat pancreas. *Regul. Pept.* **2005**, *126*, 67−71.

(14) Egido, E. M.; Rodriguez-Gallardo, J.; Silvestre, R. A.; Marco, J. Inhibitory effect of ghrelin on insulin and pancreatic somatostatin secretion. *Eur. J. Endocrinol.* **2002**, *146*, 241−244.

(15) Doi, A.; Shono, T.; Nishi, M.; Furuta, H.; Sasaki, H.; et al. IA-2b, but not IA-2, is induced by ghrelin and inhibits glucose-stimulated insulin secretion. *Proc. Natl. Acad. Sci. U.S.A.* **2006**, *103*, 885−890.

(16) Broglio, F.; Gottero, C.; Benso, A.; Prodam, F.; Destefanis, S.; et al. Effects of ghrelin on the insulin and glycemic responses to glucose, arginine, or free fatty acids load in humans. *J. Clin. Endocrinol. Metab.* **2003**, *88*, 4268−4272.

(17) Saad, M. F.; Bernaba, B.; Hwu, C. M.; Jinagouda, S.; Fahmi, S.; et al. Insulin regulates plasma ghrelin concentration. *J. Clin. Endocrinol. Metab.* **2002**, *87*, 3997−4000.

(18) Cummings, D. E.; Purnell, J. Q.; Frayo, R. S.; Schmidova, K.; Wisse, B. E.; et al. A preprandial rise in plasma ghrelin levels suggests a role in meal initiation in humans. *Diabetes* **2001**, *50*, 1714−1719.

(19) Tolle, V.; Bassant, M. H.; Zizzari, P.; Poindessous-Jazat, F.; Tomasetto, C.; et al. Ultradian rhythmicity of ghrelin secretion in relation with GH, feeding behavior, and sleep-wake patterns in rats. *Endocrinology* **2002**, *143*, 1353−1361.

(20) Toshinai, K.; Mondal, M. S.; Nakazato, M.; Date, Y.; Murakami, N.; et al. Upregulation of ghrelin expression in the stomach upon fasting, insulin-induced hypoglycemia, and leptin administration. *Biochem. Biophys. Res. Commun.* **2001**, *281*, 1220−1225.

(21) Sun, Y.; Wang, P.; Zheng, H.; Smith, R. G. Ghrelin stimulation of growth hormone release and appetite is mediated through the growth hormone secretagogue receptor. *Proc. Natl. Acad. Sci. U.S.A.* **2004**, *101*, 4679−4684.

(22) Reimer, M. K.; Pacini, G.; Ahren, B. Dose-dependent inhibition by ghrelin of insulin secretion in the mouse. *Endocrinology* **2003**, *144*, 916−921.

(23) Muller, A. F.; Janssen, J. A.; Hofland, L. J.; Lamberts, S. W.; Bidlingmaier, M.; et al. Blockade of the growth hormone (GH) receptor unmasks rapid GH-releasing peptide-6-mediated tissue-specific insulin resistance. *J. Clin. Endocrinol. Metab.* **2001**, *86*, 590−593.

(24) Svensson, J.; Lonn, L.; Jansson, J. O.; Murphy, G.; Wyss, D.; et al. Two-month treatment of obese subjects with the oral growth hormone (GH) secretagogue MK-677 increases GH secretion, fat-free mass, and energy expenditure. *J. Clin. Endocrinol. Metab.* **1998**, *83*, 362−369.

(25) Chapman, I. M.; Bach, M. A.; Van Cauter, E.; Farmer, M.; Krupa, D.; et al. Stimulation of the growth hormone (GH)-insulin-like growth factor I axis by daily oral administration of a GH secretagogue (MK-677) in healthy elderly subjects. *J. Clin. Endocrinol. Metab.* **1996**, *81*, 4249−4257.

(26) The synthesis of compounds **1** and **2** is described in the Supporting Information.

(27) Fenton, G.; Newton, C. G.; Wyman, B. M.; Bagge, P.; Dron, D. I.; et al. Hypolipidemic 2-[4-(1,1-dimethylethyl)phenyl]-4H-3,1-benzoxazin-4-ones. Structure-activity relationships of a novel series of high-density lipoprotein elevators. *J. Med. Chem.* **1989**, *32*, 265−272.

(28) Shcherbakova, I.; Balandrin, M. F.; Fox, J.; Ghatak, A.; Heaton, W. L.; et al. 3H-Quinazolin-4-ones as a new calcilytic template for the potential treatment of osteoporosis. *Bioorg. Med. Chem. Lett.* **2005**, *15*, 1557−1560.

(29) Herdemann, M.; Al-Mourabit, A.; Martin, M.-T.; Marazano, C. From a biogenetic scenario to a synthesis of the ABC ring of manzamine A. *J. Org. Chem.* **2002**, *67*, 1890−1897.

(30) Frlan, R.; Kikelj, D. Recent progress in diaryl ether synthesis. *Synthesis* **2006**, 2271−2285.

(31) Daidone, G.; Plescia, S.; Raffa, D.; Schillaci, D.; Maggio, B.; et al. Synthesis, crystallographic studies and biological evaluation of some 2-substituted 3-indazolyl-4(3H)-quinazolinones and 3-indazolyl-4(3H)-benzotriazinones. *Heterocycles* **1996**, *43*, 2385−2396.

(32) Salehi, P.; Dabiri, M.; Zolfigol, M. A.; Baghbanzadeh, M. A novel method for the one-pot three-component synthesis of 2,3-dihydroquinazolin-4(1H)-ones. *Synlett* **2005**, 1155−1157.

(33) van Niel, M. B.; Collins, I.; Beer, M. S.; Broughton, H. B.; Cheng, S. K. F.; et al. Fluorination of 3-(3-(piperidin-1-yl)propyl)indoles and 3-(3-(1-piperazinyl)propyl)indoles gives selective human 5-HT1D receptor ligands with improved pharmacokinetic profiles. *J. Med. Chem.* **1999**, *42*, 2087−2104.

(34) http://www.acdlabs.com/products/phys_chem_lab/pka/.

(35) Lipinski, C. A.; Hoffer, E. Compound properties and drug quality. *Pract. Med. Chem. (2nd ed.)* **2003**, 341−349.

(36) Holst et al. have demonstrated that recombinant GHS-R1a overexpressed in mammalian cells displays a high level of constitutive activity, the physiological relevance of which has not yet been fully understood. However, our observation that neutral antagonists promote weight loss and improve glucose homeostasis in rodents (vida infra) indicates that inverse agonism is not a prerequisite for efficacy in these models. Comparison of the effects of a strong inverse agonist with a neutral antagonist could provide further insight into the physiologic relevance of GHS-R1a constitutive activity. Holst, B.; Schwartz, T. W. Constitutive ghrelin receptor activity as a signaling set-point in appetite regulation. *Trends Pharmacol. Sci.* **2004**, *25*, 113−117.

(37) http://www.daylight.com/dayhtml/doc/clogp/index.html.

(38) Affinities for the homologous motilin receptor, the serotonine receptors 5-HT2 a, b, and c, and the L type calcium channel receptor were >1 μM for both compounds. Compound **43** was tested in a panel of overall 21 receptor assays and did not reveal any significant activities.

(39) Carai, M. A. M.; Colombo, G.; Maccioni, P.; Gessa, G. L. Efficacy of rimonabant and other cannabinoid CB1 receptor antagonists in reducing food intake and body weight: Preclinical and clinical data. *CNS Drug Rev.* **2006**, *12*, 91−99.

(40) Cummings, D. E.; Foster-Schubert, K. E.; Overduin, J. Ghrelin and energy balance: Focus on current controversies. *Curr. Drug Targets* **2005**, *6*, 153−169.

(41) Levin, B. E.; Dunn-Meynell, A. A.; Ricci, M. R.; Cummings, D. E. Abnormalities of leptin and ghrelin regulation in obesity-prone juvenile rats. *Am. J. Physiol.* **2003**, *285*, E949−E957.

(42) The synthesis of compound **47** involved a slight variation of the sequence described in Scheme 1. Its preparation is described in the Supporting Information.

(43) Serby, M. D.; Zhao, H.; Szczepankiewicz, B. G.; Kosogof, C.; Xin, Z.; et al. 2,4-Diaminopyrimidine derivatives as potent growth hormone secretagogue receptor antagonists. *J. Med. Chem.* **2006**, *49*, 2568−2578.

(44) Kelder, J.; Grootenhuis, P. D. J.; Bayada, D. M.; Delbressine, L. P. C.; Ploemen, J.-P. Polar molecular surface as a dominating determinant for oral absorption and brain penetration of drugs. *Pharm. Res.* **1999**, *16*, 1514−1519.

(45) Ertl, P.; Rohde, B.; Selzer, P. Fast calculation of molecular polar surface area as a sum of fragment-based contributions and its application to the prediction of drug transport properties. *J. Med. Chem.* **2000**, *43*, 3714−3717.

(46) Sun, Y.; Asnicar, M.; Saha, P. K.; Chan, L.; Smith, R. G. Ablation of ghrelin improves the diabetic but not obese phenotype of ob/ob mice. *Cell Metab.* **2006**, *3*, 379−386.

(47) Esler, W. P.; Rudolph, J.; Claus, T. H.; Brands, M.; Tang, W.; et al. Small-molecule ghrelin receptor antagonists improve glucose tolerance, suppress appetite, and promote weight loss. *Endocrinology*, in press.

(48) Pan, C. Q.; Buxton, J. M.; Yung, S. L.; Tom, I.; Yang, L.; et al. Design of a long acting peptide functioning as both a glucagon-like peptide-1 receptor agonist and a glucagon receptor antagonist. *J. Biol. Chem.* **2006**, *281*, 12506−12515.